Interannual variability of the ecosystem CO_2 fluxes at paludified spruce forest and ombrotrophic bog in southern taiga

Vadim Mamkin[1], Vitaly Avilov[1], Dmitry Ivanov[1], Andrey Varlagin[1], Julia Kurbatova[1]

[1]A.N. Severtsov Institute of ecology and evolution of the Russian Academy of Sciences, 33, Leninsky avenue, 119071, Moscow, Russia

Correspondence to: Vadim Mamkin (vadimmamkin@gmail.com)

Abstract. Climate warming in high latitudes impacts CO_2 sequestration of northern peatlands through the changes in production and decomposition processes. The response of the net CO_2 fluxes between ecosystems and the atmosphere to the climate change and weather anomalies can vary across the forest and non-forest peatlands. To better understand the differences in CO_2 dynamics at forest and non-forest boreal peatlands induced by changes in environmental conditions the estimates of interannual variability of the net ecosystem exchange (NEE), total ecosystem respiration (TER) and gross primary production (GPP) was obtained at two widespread peatland ecosystems – paludified spruce forest and adjacent ombrotrophic bog in the southern taiga of west Russia using 6-years of paired eddy covariance flux measurements. Both positive and negative annual and growing season air temperature and precipitation anomalies were observed in the period of measurements (2015-2020). Flux measurements showed that in spite of the lower growing season TER (332±17 …339±15 $gC \cdot m^{-2}$) and GPP (442±13…464±11 $gC \cdot m^{-2}$) rates the bog had a higher CO_2 uptake rates (NEE was -132±11…-108±6) than the forest excepting the warmest and the wettest year of the period (2020) and was an atmospheric CO_2 sink in the selected years while the forest was a CO_2 sink or source depending on the environmental conditions. Growing season NEE at the forest site was between -142±48 and 28±40 $gC \cdot m^{-2}$, TER between 1135±64 and 1366±58 $gC \cdot m^{-2}$ and GPP between 1207±66 and 1462±107 $gC \cdot m^{-2}$. Annual NEE at the forest was between -62±49 and 145±41 $gC \cdot m^{-2}$, TER between 1429±87 and 1652±44 $gC \cdot m^{-2}$ and GPP between 1345±89 and 1566±41 $gC \cdot m^{-2}$ respectively. Under the anomalously warm winter conditions with sparse and thin snow cover (2019/2020) the increased daily GPP, TER and net CO_2 uptake at the forest was observed while at the bog the changes in CO_2 fluxes between the warm and cold winters were not significant. This study

suggests that the warming in winter can increase CO_2 uptake of the paludified spruce forests of southern taiga in non-growing season.

1. Introduction

CO_2 net ecosystem exchange (NEE) between peatlands and the atmosphere is an important process of the global carbon cycle controlling the terrestrial carbon stocks and influence the climate system (Gorham, 1991; Aurela et al., 2002; Wieder, Vitt, 2006). Nothern peatlands store about 500±100 Gt of C (Yu, 2012) which is approximately equal to the global vegetation and about 20-30% of the soil carbon stocks (Friedlingstein et al., 2019). Annual CO_2 uptake of the peatlands in high latitudes are relatively small (Moore, 2002; Koehler et al, 2010) due to the low productivity and decomposition rates limited by wet anoxic conditions, low temperatures and pH as well as low nitrogen content in the peat (Wieder and Vitt, 2006; Weedon et al., 2013). However, northern peatlands are considered to be a stable sink of atmospheric CO_2 at the long time scales (Gorham, 1991; Moore, 2002; Alexandrov et al., 2020) as the carbon accumulation by GPP exceeds carbon loss through CO_2 release from total ecosystem respiration TER and from the other mechanisms i.e. methane emissions and dissolved organic carbon (DOC) runoff.

A warming trend in high latitudes is able to intensify both carbon accumulation and release processes affecting NEE as well as net ecosystem carbon balance of the northern peatlands (Loisel et al., 2021). It is suggested that growing air and peat temperatures especially under raising frequency of droughts in boreal regions can significantly increase decomposition rates and switch peatlands from CO_2 sink to CO_2 source for the atmosphere (e.g. Alm et al., 1999; Moore, 2002; Lund et al., 2012; LaFleur et al., 2015; Helbig et al., 2019; Loisel et al., 2021).

The response of the peatlands on climate change and weather anomalies may differ across the ecosystems depending on peatland type, local weather and hydrological regime as well as vegetation composition and management practices (Humphreys et al., 2006; Euskirchen et al., 2014; Petrescu et al., 2015; Holl et al., 2019; Qiu et al., 2020). Recent decades a numerous experimental studies showed a high spatial and temporal variability of CO_2 fluxes between different peatland ecosystems in high latitudes and its response to environmental factors (e.g. Alm et al., 1999; Humphreys et al., 2006; Lindroth et al., 2007; Minkkinen et al., 2018; Park et al., 2021). Previous studies reported that NEE of the peatlands is

susceptible to water table depth (WTD) dynamics, air and peat temperature variations, changes in global radiation, timing of snowmelting and peat layer thaw (Moore et al., 2006; Dunn et al., 2007; Lindroth et al., 2007; Sulman et al., 2010).

Forest and non-forest peatlands have a different features which determine the ecosystem – atmosphere carbon dioxide exchange: i.e. aboveground biomass, peat thickness, nutrient availability as well as different temperature and moisture regime of the upper peat layer (Moore, 2002; Kurbatova et al., 2013; Euskirchen et al., 2014; Beaulne et al., 2021). At the short time scales the forest peatlands (i.e. paludified forests) can have a similar carbon accumulation rates as the non-forest peatlands (i.e. bogs) but the forest peatlands have a lower CO_2 sequestration rates at the long time scales (Beaulne et al., 2021). Moreover, NEE of the forest and non-forest peatlands have their own seasonal specifics. For instance, the forest peatlands can sequestrate atmospheric CO_2 before the snowmelting and peat thaw in spring, while a thawing is necessary for the beginning of the CO_2 uptake at non-forest peatlands (Tanja et al., 2003; Euskirchen et al., 2014; Helbig et al., 2019). Therefore, the changes of the environmental conditions can influence the CO_2 fluxes at the forest and non-forest peatlands in different ways. With regard to the strong dependence of NEE on the environmental parameters variability, regional and site-specific features of the peatlands as well as its significant potential feedbacks to the climate system in response to the global warming (IPCC, 2014; Helbig et al., 2020; Loisel et al., 2021) the experimental estimates of the interannual variability of the ecosystem CO_2 fluxes at different peatlands located in the same landscape are very useful to assess the diversity of the possible effects of the weather anomalies and climate change on the ecosystem carbon dioxide exchange between the northern peatlands and the atmosphere (Lavoie et al., 2005; Ueyama et al., 2014; Park et al., 2021).

Unfortunately, in spite of a numerous experimental studies focused on ecosystem-atmosphere CO_2 fluxes in different peatland types in high-latitudes in North America (e.g. Roulet et al., 2007; Gill et al., 2017), Europe (e.g. Kurbatova et al., 2002; Lindroth et al., 2007; Minkkinen et al., 2018) and Asia (e.g. Tchebakova et al., 2015; Alekseychik et al., 2017; Park et al., 2021) there is lack of studies considering the ecosystem CO_2 fluxes at the forest and non-forest peatlands located in the same landscape and undergo the similar weather conditions (e.g. Euskirchen et al., 2014; Helbig et al., 2017; Zagirova et al., 2019).

Russian peatlands cover about one-third of the global peatland area (Vompersky et al., 2011). Approximately 15% of forest and non-forest peatlands in Russia are located in the European part of the country and belongs to the most widespread ecosystems in west Russia (Vompersky et al., 2011). However, the ecosystem flux data collected at peatlands in European Russia and available in literature (e.g. Kurbatova et al., 2002; Kurbatova et al., 2008; Zagirova et al., 2019) is very sparse and rarely cover a several years of measurements, which confines the research of the dependence between CO_2 fluxes and environmental conditions at interannual time scales.

This study is focused on CO_2 peatland-atmosphere exchange at two widespread ecosystem types in west Russia – ombrotrophic bog and paludified spruce forest located in west part of Valdai hills. The aim of the study was to analyze the interannual variability of NEE, TER and GPP at the ombrotrophic bog and paludified spruce forest located in the same landscape and to establish the response of CO_2 fluxes on interannual variability of environmental conditions using 6-years of paired eddy covariance flux measurements.

2. Methods

2.1 Study sites.

This study was conducted at paludified spruce forest (56.4615°N, 32.9221°E, 265 m a.s.l.) and adjacent ombrotrophic bog (56.4727° N, 33.0413° E, 240 m a.s.l.) located on the territory of the Central-Forest state natural biosphere reserve (CFSNBR) in the south-western part of Valdai hills in Tver region of Russia (Fig.1a). The sites are located 7.5 km apart (Fig. 1b) and characterized by very similar weather conditions.

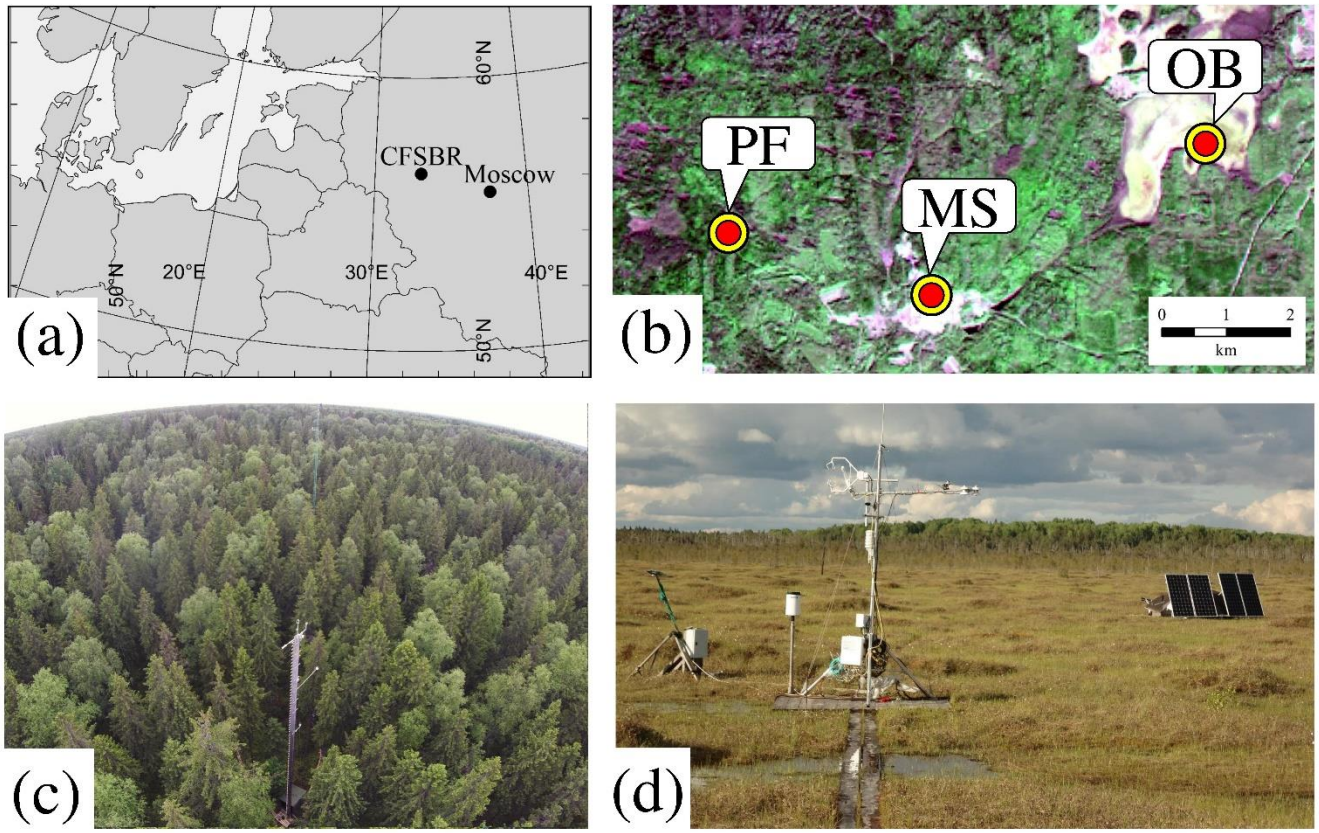

Figure 1. (a) Geographical location of the Central-Forest state natural biosphere reserve (CFSNBR); (b) location of the paludified spruce forest (PF), ombrotrophic bog "Staroselsky Mokh" (OB) and meteorological station "Lesnoy Zapovednik" (MS) on LANDSAT-8 image; photos of the eddy covariance stations at (c) PF and (d) OB sites.

The study area belongs to the humid continental climate (Dfb type in the Köppen-Geiger climate classification) (Kuricheva et al., 2017; Peel et al., 2007). According to the meteorological station "Toropets" (56.48° N, 31.63° E, 187 m a.s.l.), which is located 80 km to west from the reserve, mean air temperature at 2 m height for the period 1991-2020 was 5.7°C (-5.9 °C in January and 18.2 °C in July). Long-term mean annual precipitation (1991-2020) measured at meteorological station "Lesnoy Zapovednik" (56.50° N, 32.83° E, 240 m a.s.l.) – the nearest meteorological station to the study area was 778 mm (continuous air temperature data from "Lesnoy Zapovednik" meteostation for 1991-2020 period

is not available). Soil surface is typically covered by snow from mid-November to late March - early April (Desherevskaya et al., 2010) and the growing season calculated as the number of days between the first 5-day period with the mean daily air temperatures above 5°C (start of the growing season) to the first 5-day period with the mean daily air temperatures below 5°C (end of the growing season) following (Urban SIS, 2018; Buitenwerf et al, 2015; Donat et al, 2013; Mueller et al, 2015) lasts 182 days on average (since 12 Apr. to 11 Oct.). Annual precipitation in the study region exceed potential evapotranspiration (PET), that determines excessive moistening conditions (Mamkin et al., 2019). The climate moisture index (CMI) calculated as the ratio of annual precipitation to annual potential evapotranspiration and ranged between -1 and 1 (Wilmott, Feddema, 1992) is 0.3 - 0.4 (Novenko et al., 2015; Mamkin et al., 2019). In the recent 30 years a positive trend of air temperature (+0.73 °C per10 years) and precipitation (+3.6 mm·month^{-1} per 10 years) was detected at the meteorological stations "Toropets" and "Lesnoy Zapovednik" respectively.

The vegetation of the reserve is represented by typical plant communities of southern taiga, which are widespread at the plains in the north part of Eastern Europe (Mamkin et al., 2019; Schulze et al., 2002; Vygodskaya et al., 2002). Excessive moistening coupled with spread of glacial clay soils at the territory make the study area favourable to paludification processes and peat formation. Large areas of the CFSNBR are covered by fens, bogs and paludified forests (Schulze et al., 2002; Puzachenko et al., 2014). The paludified spruce forest (PF) named as RU-Fyo in FLUXNET database is located in a shallow depression (Kurbatova et al., 2013) on the peaty podzolic gley soils. PF is an old (with age up to 200 years) forest with Norway spruce (*Picea abies* - 86%) and white birch (*Betula pubescens* - 14%) and undergrowth dominated by Girgensohn's sphagnum (*Sphagnum girgensohnii* L.) and blueberry (*Vaccinium myrtillus* Russ.) (Milyukova et al., 2002; Kurbatova et al., 2008; Kuricheva et al., 2017). The mean tree height is 16.9±6.4 m (±SD) with mean diameter at breast height (DBH) 21.6±8.9 cm (±SD) and undergrowth is about 0.3 m. Average leaf area index (LAI) at PF site is 3.5. The thickness of the peat layer at the site is 60 cm with most of the root biomass at the depth about 30 cm. The ground water table is usually close to the surface. Peat soils have a poor soil aeration, low pH (3.5–3.8) and low nitrogen content (0.5–9.9 kg ha^{-1}) (Kurbatova et al., 2013; Milyukova et al., 2002; Vygodskaya et al., 2002).

The "Staroselsky Mokh" site (OB) named as RU-Fy4 in FLUXNET database is an old (up to 9000 years) ombrotrophic bog and has an area about 6 km^2 (Ivanov et al., 2021). Bog's vegetation is represented by different plant communities associated with topography microforms (i.a. ridges, hummocks and hollows). Vegetation of ridges and hummocks are dominated by different herbaceous species: *Drosera rotundifolia* L., *Rhynchospora alba* (L.) Vahl., *Eriophorum vaginatum* L.; shrubs: *Chamaedaphne calyculata* (L.) Moench, *Andromeda polifolia* L., *Rhododendron tomentosum* Harmaja, *Vaccinium oxycoccos* L. and mosses: *Sphagnum fuscum* (Schimp.) H. Klinggr., *S. medium* Limpr., *S. angustifolium* (C.E.O. Jensen ex Russow) C.E.O. Jensen. Vegetation of hollows is dominated by herbs: *Scheuchzeria palustris* L., *Rhynchospora alba* (L.) Vahl, *Carex limosa* L., *Drosera anglica* Huds., *Eriophorum vaginatum* L. and mosses: *Sphagnum fallax* (H. Klinggr.) H. Klinggr., *S. majus* (Russow) C.E.O. Jensen, *S. cuspidatum* Ehrh. ex Hoffm., *S. balticum* (Russow) C.E.O. Jensen, *Odontoschisma fluitans* (Nees) L. Söderstr. & Váňa, *Gymnocolea inflata* (Huds.) Dumort. (Ivanov et al., 2021). Bog edges are covered by trees, predominantly by Scots pine (*Pinus sylvestris*) with tree heights up to 10-13 m. In the central part of the bog small pine trees (within 2-5 m height) grow on some ridges.

Average peat layer thickness at OB site is 3.2 m with maximum of 5.5 m (Ivanov et al., 2021). Ground water level is typically 30 cm below the surface at ridges and hummocks and 10 cm above the surface at hollows.

2.2 Measurements

Flux stations at PF and OB sites have a standard instrumentation for FLUXNET network. Flux measurements at PF site started in 1998 (Kurbatova et al., 2013). Eddy covariance instruments are mounted on the top of 29 m tower located in the central part of the ecosystem (Fig. 1c). Flux measurements were obtained using 3-D sonic anemometer Gill Solent R3 (Gill Instruments, UK) and closed-path CO_2/H_2O gas analyzer LI-6262-3 (LI-COR Inc., USA). Eddy covariance data was collected on the flash-drive using personal computer with EddyMeas data acquisition software (Kolle and Rebmann, 2007). Global radiation was measured using radiometer CNR4 (Kipp & Zonen B.V., Netherlands) at 28 m height. Air temperature and relative humidity measurements were carried out at 28 m height using humidity and temperature probe HMP35D (Vaisala Inc., Finland) as well as atmospheric

pressure using PTB101B (Vaisala Inc., Finland) at the same height. Precipitation was measured using tipping bucket rain gauge 52202H (R. M. Young Company, USA) at 20 m height. WTD was measured using pressure transducer CS451 (Campbell Sci. inc., USA) at 1.8 m depth. Soil temperature measurements at 5 cm depth were obtained using 3 reflectometers CS650 (Campbell Scientific, USA). Meteorological data was collected every 10 s using data logger Dl 3000 (Delta-T Devices Ltd, UK).

Eddy covariance and meteorological instruments at OB site were installed in 2015 at 3.5 m tripod which was placed in the central part of the bog (Fig. 1d). Instruments for flux measurements included 3-D sonic anemometer CSAT-3 (Campbell Sci. Inc., USA) and open-path CO_2/H_2O gas analyzer LI-7500A (LI-COR Inc., USA) mounted at 2.85 m height. Eddy covariance data was collected using LI-7550 Analyzer interface unit (LI-COR Inc., USA) at frequency of 10 Hz.

Additionally, global radiation at OB site was measured with 4-component radiometer NR01 (Hukseflux Thermal Sensors, The Netherlands) at 2.5 m height. Air temperature, relative humidity and atmospheric pressure was measured using weather transmitter HMP155 (Vaisala Inc., Finland) at 2 m height. Precipitation was measured by rain gauge Young 52202 (R. M. Young Company, USA) at 1 m height near the tripod. WTD measurements were obtained using submersible pressure transducer CS451 (Campbell sci. Inc., USA) installed 1.67 m below the surface. Temperature of the peat layer at 5 cm depth was measured by 3 temperature probes T109 (Campbell sci. Inc., USA) placed in hollow, in hummock and between them. Meteorological data was collected every 1 min using data logger CR1000 (Campbell sci. Inc., USA). The Moscow time (UTC+3) was used for data storage.

2.3 Data processing and statistical analysis

This study is based on eddy covariance and meteorological data obtained at PF and OB sites in 2015-2020. Net ecosystem exchange (NEE) at two sites was calculated for 30-min intervals using EddyPro software (LI-COR Inc., USA) with all required statistical tests and corrections. Footprint was estimated using Kljun et al. (2004) model. 0-2 quality flags (Mauder and Foken, 2006) were assigned to calculated fluxes. All fluxes with quality flag 2 were removed from the analysis following the recommendations on the data quality assessment (Mauder et., 2013). Additionally, all data containing the spikes, collected under rain and dew events as well as under low turbulence were also filtered out. Storage terms were

calculated using one-point approach (Greco, Baldocchi, 1996) and added to CO_2 flux values. u*-filtering of NEE, gap-filling and NEE partitioning into GPP and TER was carried out using REddyProc package (Wutzler et al., 2018).

Mean annual u*-threshold for NEE at PF site varied between 0.354 and 0.529 $m \cdot s^{-1}$ and between 0.058 and 0.064 $m \cdot s^{-1}$ at OB site. Uncertainty of NEE, TER and GPP associated with the random error in the measured fluxes, u*-threshold estimation, gap-filling and flux partitioning procedures was calculated using REddyProc package (Wutzler et al., 2018) as standard deviation (SD) of the flux values. The aggregated random uncertainty of the seasonal and annual sums of the CO_2 fluxes was obtained considering the autocorrelation between the residuals using empirical autocorrelation function (Zięba, Ramza, 2011).

The statistical significance of the changes in CO_2 fluxes between the years of measurements at PF and OB sites was estimated using Mann-Whitney U-test (M-W U-test) and Kruskal-Wallis ANOVA (K-W test) with Dunn's post hoc test as the daily TER, GPP and NEE values were not normally distributed (Shapiro-Wilk's test, $p<0.05$).

2.4 Parametrization the dependence of CO_2 fluxes on environmental factors

The main ambient factors controlling CO_2 fluxes at the terrestrial ecosystems under the absence of water stress are soil and air temperatures and the global radiation (Rg). To research how TER and GPP rates varied following the changes in the environmental conditions we considered the dependence of the night-time TER on soil and air temperature and dependence of GPP on Rg. Only original NEE data was used for the calculation of TER and GPP for this analysis. To describe the dependence of TER on air and soil temperature a widely used Q_{10} function was implemented. Q_{10} and R_{10} coefficients were calculated following (Pavelka et al., 2007):

$$Q_{10} = \exp(10 \cdot \alpha) \quad (1)$$

where, α is an empirical parameter taken from the following equation:

$$Ln(TER) = \alpha \cdot T + \gamma \quad (2)$$

Where T is soil or air temperature [°C] and γ is an empirical parameter of the equation.

The dependence between GPP and Rg [$W \cdot m^{-2}$] was described using well-known Michaelis - Menten hyperbolic light-response curve:

$$GPP = \frac{\alpha \cdot \beta \cdot Rg}{\alpha \cdot Rg + \beta} \quad (3)$$

Where α and β are empirical parameters of the equation. α is a canopy light utilization parameter [$\mu mol \cdot J^{-1}$] and β is a maximum CO_2 uptake at light saturation [$\mu mol \cdot m^{-2} \cdot s^{-1}$] (Matthews et al., 2017).

2.5 Additional data

Analysis of the weather conditions in the period 2015-2020 as well as calculation of the mean long-term values of the meteorological parameters is based on the data collected at the two meteorological stations. Mean air temperature data downloaded from the RIHMI-WDC database (http://aisori-m.meteo.ru) measured at "Toropets" station was used. Only precipitation and snow cover data collected at the nearest to the sites meteorological station "Lesnoy Zapovednik" was used considering the non-uniform spatial distribution of the precipitation in the region and the lack of air temperature data collected at "Lesnoy Zapovednik" station.

3. Results

3.1 Meteorological conditions

Six years of measurements showed a wide interannual variability of the meteorological conditions (Fig.2). According to the data from the meteorological station "Toropets" mean annual air temperature in the period 2015-2020 was higher than the long term mean value for the period 1991-2020 (Table 1) excepting 2017 when the mean annual air temperature anomaly was not observed. Analysis of the precipitation data from meteorological station "Lesnoy Zapovednik" showed that annual precipitation in 2015 and 2018 was lower than the mean long-term annual precipitation sum and higher in 2016, 2017, 2019 and 2020. Mean air temperature calculated for the long-term growing season period (LTGS, 12 Apr. – 11 Oct.) was lower in 2015, 2017 and 2019 than the long-term mean for the same period and higher in 2016, 2018 and 2020. LTGS precipitation was lower in 2015 and 2018 and higher in 2016, 2017, 2019 and 2020. Growing

season precipitation correlated with annual precipitation sums but proportion between them increased from 45% in 2015 to 65% in 2020.

Therefore, the environmental conditions in the selected years were notably different. The 2017 was the coldest year of the period with the lowest global radiation and relatively high annual and growing season precipitation. In contrast, 2018 was relatively warm with highest global radiation and lowest annual and growing season precipitation. The warmest and the wettest year (as well as growing season) of the period was 2020.

All winters (Nov.-Mar.) of the selected period (2015-2020) excepting winter 2017/2018 were warmer in relation to the long-term means but the mean winter air temperatures were primarily negative (Table 2). Positive mean winter air temperature was observed in winter 2019/2020. Snow cover formed from late October to beginning of January and was melting in April with snow depth reaching 40 cm. In winter 2019/2020 snow cover was anomalously sparse and thin (0-10 cm) and was observed only since the first week of January to mid-February.

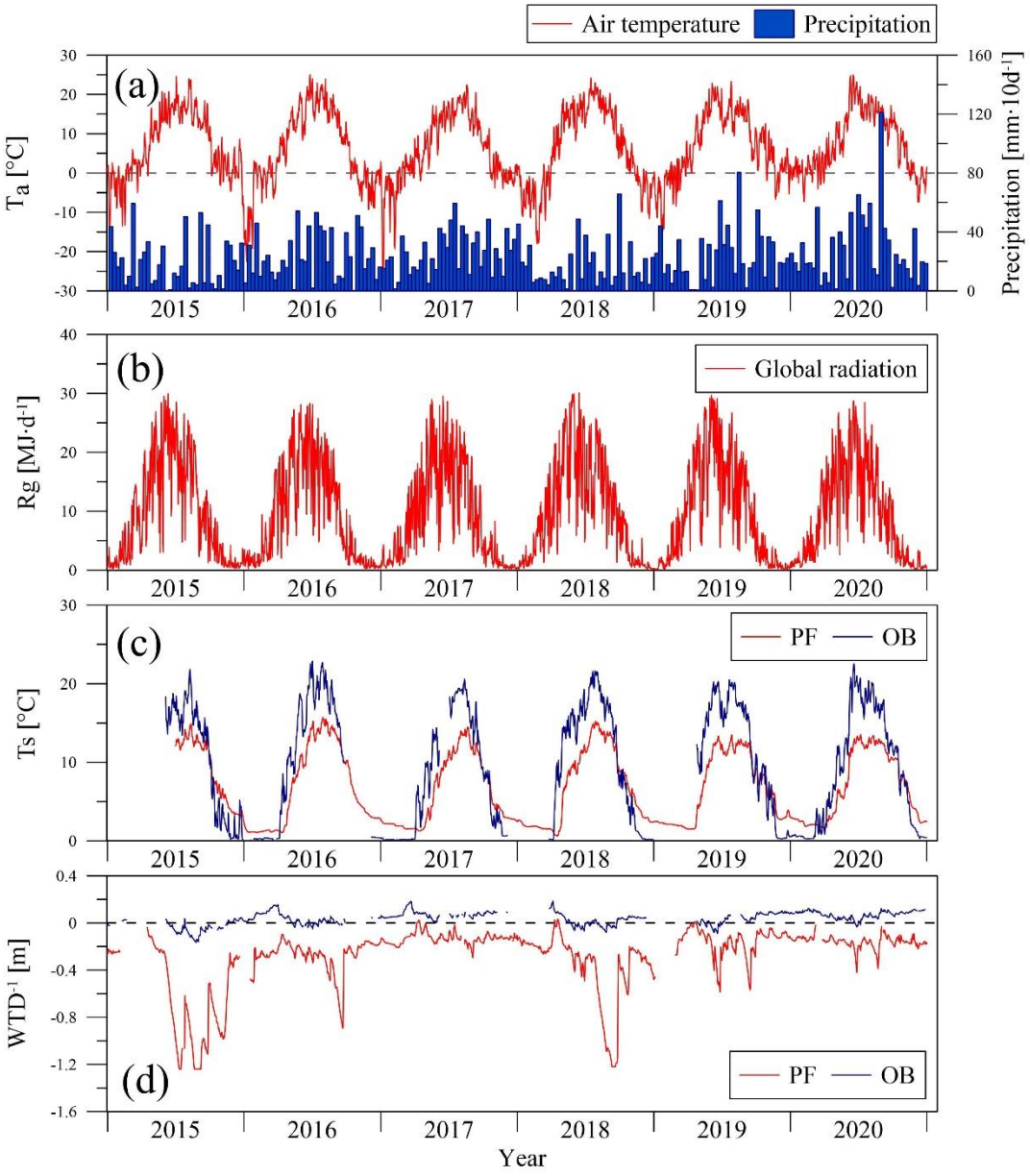

Figure 2 Seasonal variation of mean daily air temperature (T_a) at meteorological station "Toropets", 10-day precipitation sums at meteorological station "Lesnoy Zapovednik" (MS) (a), daily global radiation sums at paludified forest (PF) (b), mean daily soil temperature at 5 cm depth (T_s) (c) as well as inverse value of water table depth (WTD^{-1}) at PF and ombrotrophic bog (OB) sites correspondingly in the period 2015-2020.

Table 1. Meteorological conditions in the period 2016-2020: mean annual air temperature (T_a), mean air temperature calculated for the long-term growing season (LTGS, 12 Apr – 11 Oct) ($T_{a,g.s.}$) and growing season length (GSL) at meteorological station "Toropets", annual sum of precipitation (Pr) and sum of precipitation calculated for LTGS period ($Pr_{g.s.}$) at meteorological station "Lesnoy Zapovednik" (MS) as well as long-term (1991-2020) mean values of T_a, $T_{a,g.s}$, Pr and $Pr_{g.s}$ with standard deviations (±SD); annual sums of global radiation (Rg), mean annual soil temperature (T_s) at 5 cm depth and mean annual water table depth at paludified forest (PF).

	2015	**2016**	**2017**	**2018**	**2019**	**2020**	**Long-Term**
T_a [°C]	6.8	5.8	5.7	6.0	7.0	7.6	5.7±0.8
$T_{a, g.s.}$ [°C]	13.5	14.3	12.3	14.8	13.4	13.8	13.6±0.8
GSL [days]	180	187	174	194	172	178	182
Pr [mm]	671	864	956	560	848	992	778±123
$Pr_{g.s.}$ [mm]	300	479	562	343	492	640	445±114
Rg [MJ·m^{-2}]	3592	3402	3249	3659	3456	3333	
T_s [°C]	9.0*	6.7	6.0	6.7	6.6	6.7	
WTD [m]	0.63	0.28	0.13	0.37	0.16	0.16	

*- T_s was calculated for 03.07 – 31.12 2015.

Table 2. Mean air temperature in winters (1Nov – 31 Mar) of 2015-2020 period as well as mean long-term value of air temperature at meteorological station "Toropets" [°C] with standard deviation (±SD).

2015/2016	**2016/2017**	**2017/2018**	**2018/2019**	**2019/2020**	**Long-Term**
-2.2	-3.0	-3.5	-2.4	1.3	-3.5±1.9

Soil temperature and water table depth dynamics at the sites were influenced by seasonal and interannual changes of the weather conditions. Mean annual soil temperature at 5 cm depth was higher at OB site than at PF site in growing season of the each year: mean daily soil temperature in summer reached 22.9 °C while at PF site it didn't exceed 13.5 °C. On the contrary, in winter soil temperature at PF site was

higher than at OB site: mean daily soil temperature in winter varied between 1 and 3 °C at PF site while it reached 0 °C at OB site. WTD at the sites had a seasonal variation, so the minimal values were very similar and observed after the snowmelting in spring of each year (-0.20 m at OB and -0.16 m at PF), then WTD usually increased to late August and September to 1.2 m at PF site and to 0.15 m at OB site. In spite of the difference in precipitation between the years ground water at OB site was close to surface, when WTD at PF site increased in summer to it's maximal values in the years with lower precipitation and was within 0.40-0.50 m in the relatively wet years.

3.2 Ecosystem CO_2 fluxes

Eddy covariance CO_2 flux measurements showed a wide seasonal and interannual variability connected with the changes in environmental conditions among the study period (2015 – 2020). During the 6 years of measurements CO_2 uptake at PF site tended to increase. PF was a CO_2 source in 2015, 2016, 2017 and 2019 and a CO_2 sink in 2018 and 2020 (Table 3). Annual sums of CO_2 at OB site were obtained only for 2020 when OB was a stronger CO_2 sink than PF site, but the annual sums of GPP and TER was lower in 3.0 - 3.5 times respectively. Mean annual GPP/TER ratio at PF site varied between 0.85 – 1.04 in the period 2015 – 2020 and was 1.23 at OB site in 2020. At PF site mean GPP/TER ratio in 2020 was significantly higher than in the previous years (K-W test, $H=37.508$, $n=2192$, $p<0.001$, post hoc Dunn's test $p<0.05$), moreover the difference between GPP/TER ratio in other years was not significant. Maximal and minimal annual NEE, TER and GPP at PF site were not correspondent with maximal and minimal GSL. Minimal values of annual GPP at PF site were observed in the years with relatively low air temperatures (2016 and 2017) and the relatively high values of annual GPP corresponded to the years with high global radiation (2015, 2018 and 2019). Annual sums of TER at PF site were minimal in the years with maximal precipitation and correspondingly with the minimal mean annual WTD. However, due to the high uncertainty of annual TER and GPP at PF site, comparable with its interannual variability, it is challenging to attribute changes in annual sums of TER and GPP to the environmental conditions in the particular years of the period.

The annual TER and GPP were mainly determined by its growing season sums. Growing season sums (Table 4) of TER and GPP at PF site (calculated for the long-term climatic growing season 12.04-11.10)

made up 84-86% and 90-92% respectively in 2015-2019. In 2020 due to the anomalously warm winter 2019/2020 characterized by sparse and thin snow cover growing season sums were 76% of annual TER and 86% of annual GPP. At OB site growing season sums in 2020 were 81% of annual TER and 92% of annual GPP. Comparison of the growing season NEE for 2016, 2019 and 2020 at two sites showed that OB site was a CO_2 sink in all selected years while PF site was a CO_2 source in 2016, moreover NEE at OB site was lower than at PF site in spite of the lower GPP rates in 2016 and 2019 but in 2020 lower growing season NEE at PF site was detected (Table 4) The GPP/TER ratio in growing season was 0.98 – 1.12 at PF site and 1.32 – 1.40 at OB site.

Similarly, the lowest winter sums (01 Nov – 31 Mar) of NEE at PF site were detected in relatively warm years that is mostly connected with increased GPP. Winter GPP in the warmest winter was higher than in the coldest one on 65%: 43±26 (±SD associated with flux uncertainty) $gC \cdot m^{-2}$ in winter 2017/2018 and 123±17$gC \cdot m^{-2}$ in winter 2019/2020) while TER increased on 28% (149±27 $gC \cdot m^{-2}$ in winter 2017/2018 and 206±16 $gC \cdot m^{-2}$ in winter 2019/2020). At OB site all main components of NEE (TER and GPP) were lower than at PF site in winter. We compared the winter sums of carbon dioxide fluxes at PF and OB sites for two winter seasons: winter 2015/2016 with thick and continuous snow cover and anomalously warm winter 2019/2020 with thin and sparse snow cover. It was obtained that NEE at OB site in winter 2019/2020 was slightly higher (40±4 $gC \cdot m^{-2}$) than in winter 2015/2016 (34±5 $gC \cdot m^{-2}$) while NEE at PF site in winter 2019/2020 (83±16 $gC \cdot m^{-2}$) was lower than in winter 2015/2016 (115±17 $gC \cdot m^{-2}$). The response of CO_2 exchange on anomalously warm weather conditions in winter 2019/2020 at PF and OB sites was different. At PF site GPP/TER ratio increased from 0.38 in winter 2015/2016 to 0.60 in winter 2019/2020 but at OB site it slightly decreased from 0.38 to 0.37. At PF site GPP and TER were higher in winter 2019/2020 on 42 and 9% respectively and at OB site GPP increased on 8% and TER on 12%. Mean daily TER and GPP values at PF site in winter 2019/2020 were significantly higher than in winter 2015/2016 (M-W U-test, n=152; U=9355, Z=-2.866, p=0.004 for TER and U=8170, Z=-4.413, p<0.001 for GPP) and NEE was lower (M-W U-test, n=152, U=9585, Z=2.566, p=0.010). At OB site a significant difference in mean daily TER (M-W U-test, n=152, U=10570, Z=-1.281, p=0.200), GPP (M-W U-test, n=152, U=11497, Z=0.07112, p=0.943) and NEE (M-W U-test, n=152, U=10499, Z=-1.374, p=0.170) between the winters was not found. Therefore, the warm winter lead to the substantial changes in the

daily and seasonal CO_2 fluxes at the paludified forest, especially in GPP and relatively small changes in the daily and seasonal CO_2 fluxes at the bog site.

Table 3 Annual sums of the net ecosystem exchange (NEE), total ecosystem respiration (TER) and gross primary production (GPP) with uncertainty estimates associated with random error in the measured fluxes, u*-threshold estimation, gap-filling and flux partitioning procedures (±SD) and GPP/TER ratio at the paludified forest (PF) in the period 2015 – 2020 and the ombrotrophic bog (OB) in 2020.

	2015	**2016**	**2017**	**2018**	**2019**	**2020**	**2020 (OB)**
NEE [gC·m^{-2}]	70±40	145±41	21±48	-30±40	39±42	-62±49	-95±12
TER [gC·m^{-2}]	1636±66	1652±44	1366±92	1537±43	1631±118	1429±87	410±20
GPP [gC·m^{-2}]	1566±76	1408±45	1345±89	1566±41	1592±112	1491±102	505±13
GPP/TER	0.96	0.85	0.99	1.02	0.98	1.04	1.23

Table 4. Growing season (calculated for long-term mean growing season 12.04 – 11.10) sums of net ecosystem exchange (NEE), total ecosystem respiration (TER), gross primary production (GPP) with uncertainty estimates associated with random error in the measured fluxes, u*-threshold estimation, gap-filling and flux partitioning procedures (±SD) and GPP/TER ratio at the paludified forest (PF) and at the ombrotrophic bog (OB) in the period 2015 – 2020.

	2015	**2016**		**2017**	**2018**	**2019**		**2020**	
	PF	**PF**	**OB**	**PF**	**PF**	**PF**	**OB**	**PF**	**OB**
NEE [gC·m^{-2}]	-43±39	28±40	-108±6	-72±38	-135±38	-78±39	-120±8	-142±48	-132±11
TER [gC·m^{-2}]	1366±58	1317±41	334±10	1135±64	1308±39	1384±110	339±15	1140±83	332±17
GPP [gC·m^{-2}]	1409±69	1289±42	442±13	1207±66	1443±38	1462±107	458±10	1282±100	464±11
GPP/TER	1.03	0.98	1.32	1.06	1.10	1.06	1.35	1.12	1.40

Lower GPP and TER rates at OB site in comparing with GPP and TER at PF site were also detected in seasonal variability in all years of measurements (Fig. 3). Maximal daily sums of TER and GPP were observed in summer: TER reached 19 $gC \cdot m^{-2} \cdot d^{-1}$ and GPP 18 $gC \cdot m^{-2} \cdot d^{-1}$ at PF site, while at OB site TER didn't exceed 6 $gC \cdot m^{-2} \cdot d^{-1}$ and GPP 7 $gC \cdot m^{-2} \cdot d^{-1}$ respectively. As a result, seasonal amplitude of NEE at PF site was more pronounced than at OB site and the daily sums of NEE ranged between 7 and -7 $gC \cdot m^{-2} \cdot d^{-1}$ at PF site and between 1 and -3 $gC \cdot m^{-2} \cdot d^{-1}$ at OB site.

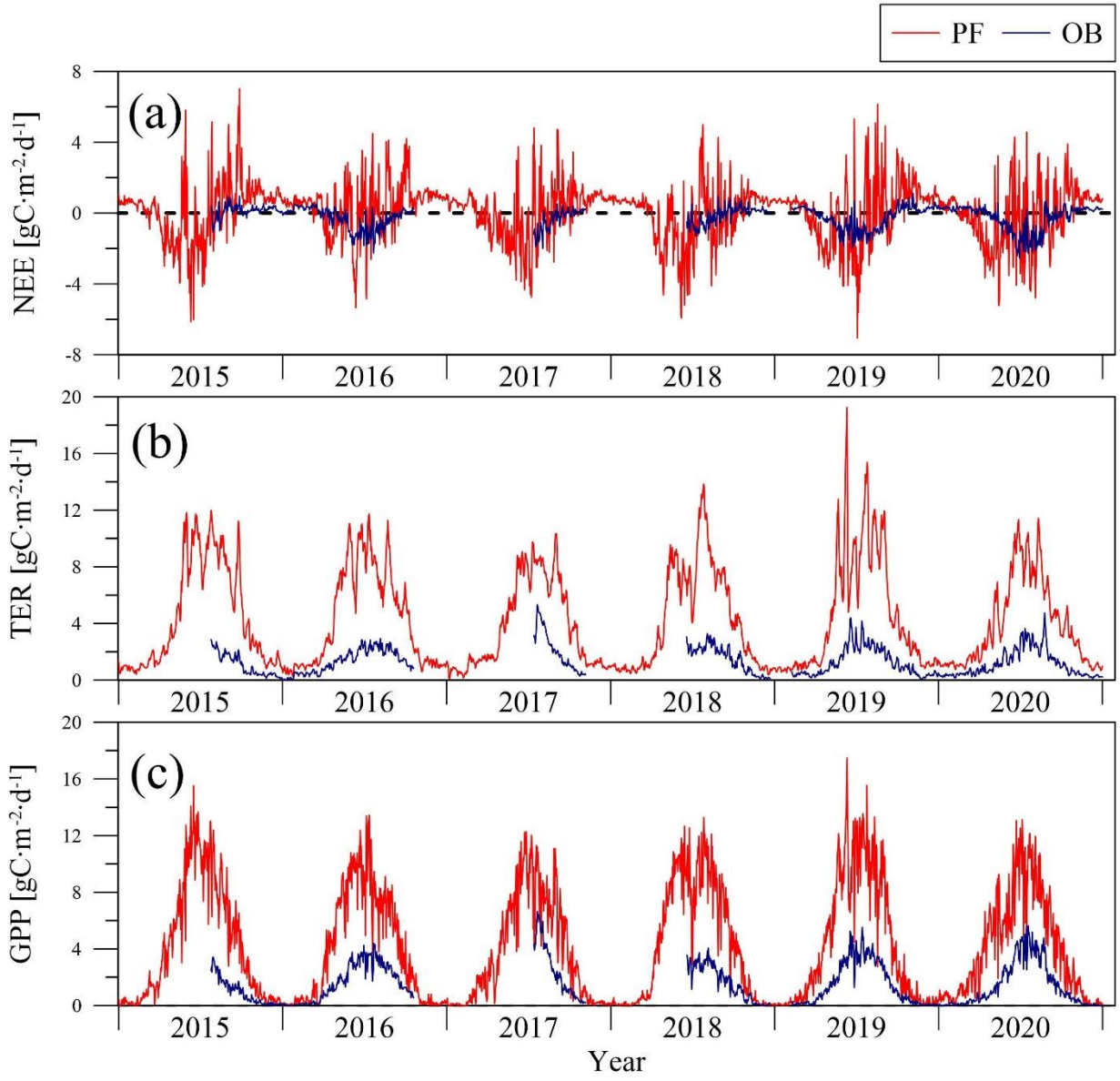

Figure 3 Seasonal variation of the net ecosystem exchange (NEE) (a), total ecosystem respiration (TER) (b) and gross primary production (GPP) (c) at paludified forest (PF) and ombrotrophic bog (OB) sites in the period 2015-2020.

In 2015-2019 period PF became a sink of atmospheric CO_2 in March (3-7 weeks before the start of the growing season calculated using mean daily air temperature data) and CO_2 source in late September –

mid October. OB site became a sink after snow melting in late April (2-4 weeks after the start of the growing season) – first decade of May and a CO_2 source in September. In the warmest year - 2020 at PF site the first days with daily NEE<0 were observed in mid-February (10 weeks before the start of the growing season) while at OB site only in the end of May (5 weeks after the start of the growing season). The shift of compensation point due to the positive temperature anomaly and lack of snow cover in winter and early spring to the earlier dates at PF site and later dates at OB site can be explained by the difference in vegetation composition and its phenology. Primary production of the conifer trees at PF site in February and March is limited by low air temperatures and the positive temperature anomaly triggered early CO_2 uptake at the forest site thus the GPP at PF site grew faster than TER. At OB site the lack of snow lead to the fast heating of the upper peat layer and consequently TER increased faster than GPP. In spite of the higher CO_2 uptake at OB site, time period when the PF site was a sink of atmospheric CO_2 was longer primarily in spring. Therefore, weather conditions in spring play an important role in the differences between NEE at paludified spruce forest and ombrotrophic bog.

3.3 Environmental controls of CO_2 fluxes

The main components of NEE (TER and GPP) varied during the period (2015-2020) following the changes in the different environmental factors. The TER rates at the sites were sensitive to the soil and air temperatures. We used Q_{10} function (Eq.1) for parametrization the dependence of TER on air and soil temperatures at PF and OB sites (Fig. 4). Only original night-time data of NEE collected in 12 Apr. – 11 Oct. period was used for the analysis. Mean night-time soil temperature at OB site varied in the wider range than at PF site from 3 ℃ and reaching 25 ℃, while at PF site it was between 0 and 15 °C. Air temperature variations at night were very similar at two sites. TER rates in the presented soil and air temperature ranges had a different magnitude at the sites. TER at PF site reached 16 $\mu mol \cdot m^{-2} \cdot s^{-1}$ while TER at OB site didn't exceed 6 $\mu mol \cdot m^{-2} \cdot s^{-1}$, moreover TER at PF site was on average higher than at OB site within the whole presented air and soil temperature ranges.

Maximal Q_{10} values at PF and OB sites were observed when soil temperature was used for Q_{10} coefficient calculation, but Q_{10} values was higher at PF site than at OB site if Q_{10} is calculated using soil temperature and higher at OB site if air temperature is used for calculation (Table 5). Similarly, maximal R_{10}

coefficient at PF site was obtained using soil temperature and using air temperature at OB site. Regardless of soil or air temperature was used, R_{10} at PF site was higher than at OB site. The residuals of the Q_{10} models showed a weak dependence on WTD (Fig. 5).

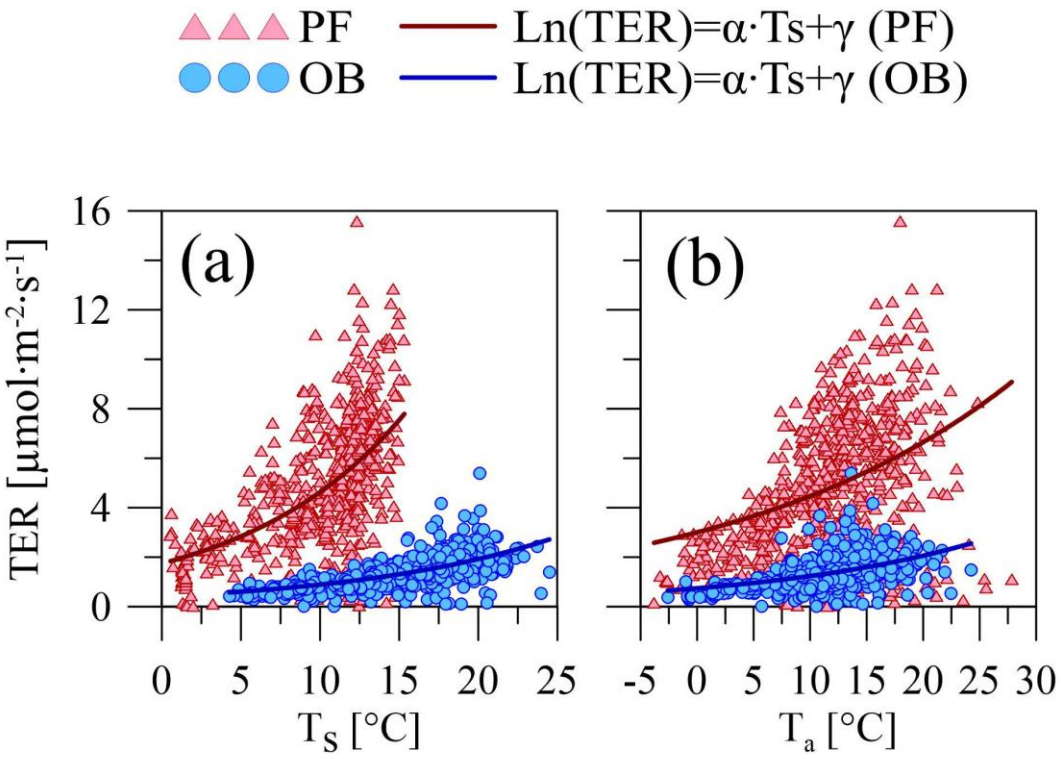

Figure 4 Relationship between the mean night-time ecosystem respiration (TER) and (a) soil (T_s) and (b) air temperature (T_a) at paludified forest (PF) and ombrotrophic bog (OB) sites in the period 12 Apr. – 11 Oct. 2015 – 2020 approximated using Q_{10} function (Eq. 1).

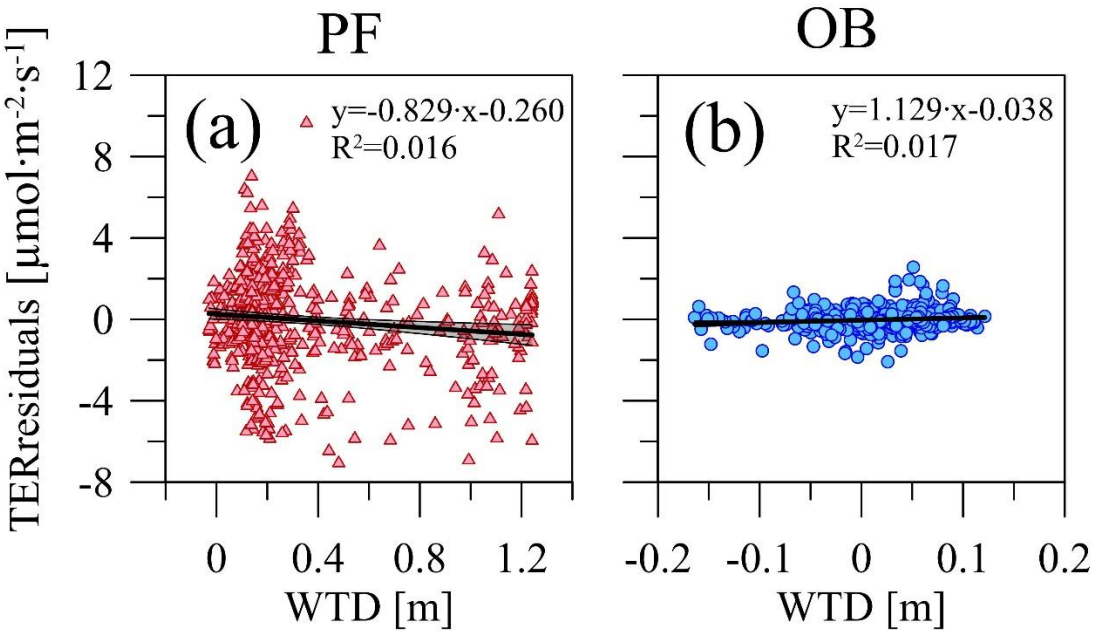

Figure 5 Relationship between the residuals of the Q_{10} model (Figure 4 a and Table 5) calculated using soil temperature and WTD at (a) paludified forest (PF) and (b) ombrotrophic bog (OB) with linear fit and its 95% confidence interval.

Table 5. Parameters α and γ of the Eq. (2) and R^2 ($p<0.01$) as well as Q_{10} and R_{10} coefficients calculated using soil (T_s) and air (T_a) temperature at paludified forest (PF) and ombrotrophic bog sites (OB).

	α	**γ**	**R^2**	**Q_{10}**	**R_{10} [µmol·m^{-2}·s^{-1}]**
PF (T_s)	0.098	0.556	0.289	2.66	4.65
OB(T_s)	0.077	-0.883	0.431	2.16	0.89
PF(T_a)	0.040	1.100	0.174	1.49	4.48
OB(T_a)	0.051	-0.297	0.261	1.67	1.24

To represent the dependence of GPP at the sites to changes in Rg we used the hyperbolic light-response curve (Eq. 3). Only 30-min GPP values calculated from original NEE data was taken for the analysis. To

show the seasonal and interannual variations of the curve parameters we considered the data in different months (April, July and October) for anomalously cool and wet growing season 2017 and anomalously warm and dry growing season 2018 (Fig. 6).

April is a beginning of the growing season and characterized by wide range of Rg and comparatively narrow range of GPP. Unfortunately, lack of the original NEE data at OB site in April didn't allow us to compare light-response curves parameters at the two sites for this month. July is the middle of the growing season, when Rg and GPP are relatively high. In the end of the growing season (October) both GPP and Rg had a relatively narrow range of variation. It is important to note that GPP at OB site was lower than at PF site in all months of the selected years that largely determined the difference in the curves' parameters between the sites due to the almost equal Rg (difference of daily sums between the sites was on average ±3%).

Analysis of the light-response curves (Table 6) showed that in relatively warm April 2018 α coefficient, (which refers to sensitivity of GPP to Rg) was lower than in relatively cold April 2017, but β coefficient (which denotes the saturation point of the curve) was higher in April 2018. In July α and β coefficients at PF site were higher in the relatively warm 2018 and in the relatively cool 2017 at OB site. In July 2017 α at PF site was lower than at OB site, but β was relatively higher. In July 2018 both α and β parameters were higher at PF site. In October 2017 and 2018 α and β were also higher at PF site and the highest values of α at PF and OB sites were detected in October 2017 while highest β in October 2018.

Additionally we compared the light response curves for March (2018 and 2020) – the last winter months in anomalously cold and snowy winter 2017/2018 and anomalously warm winter 2019/2020 with sparse and thin snow cover at PF site (Fig. 7). Due to the low GPP values it was quite difficult to establish the dependence between GPP and Rg in March 2018 while the sensitivity of GPP to changes in Rg was pronounced in March 2020 with relatively high GPP in the whole range of Rg, especially at high Rg values. It demonstrate the difference in response of GPP to interannual changes in environmental conditions at the paludified forest in early spring.

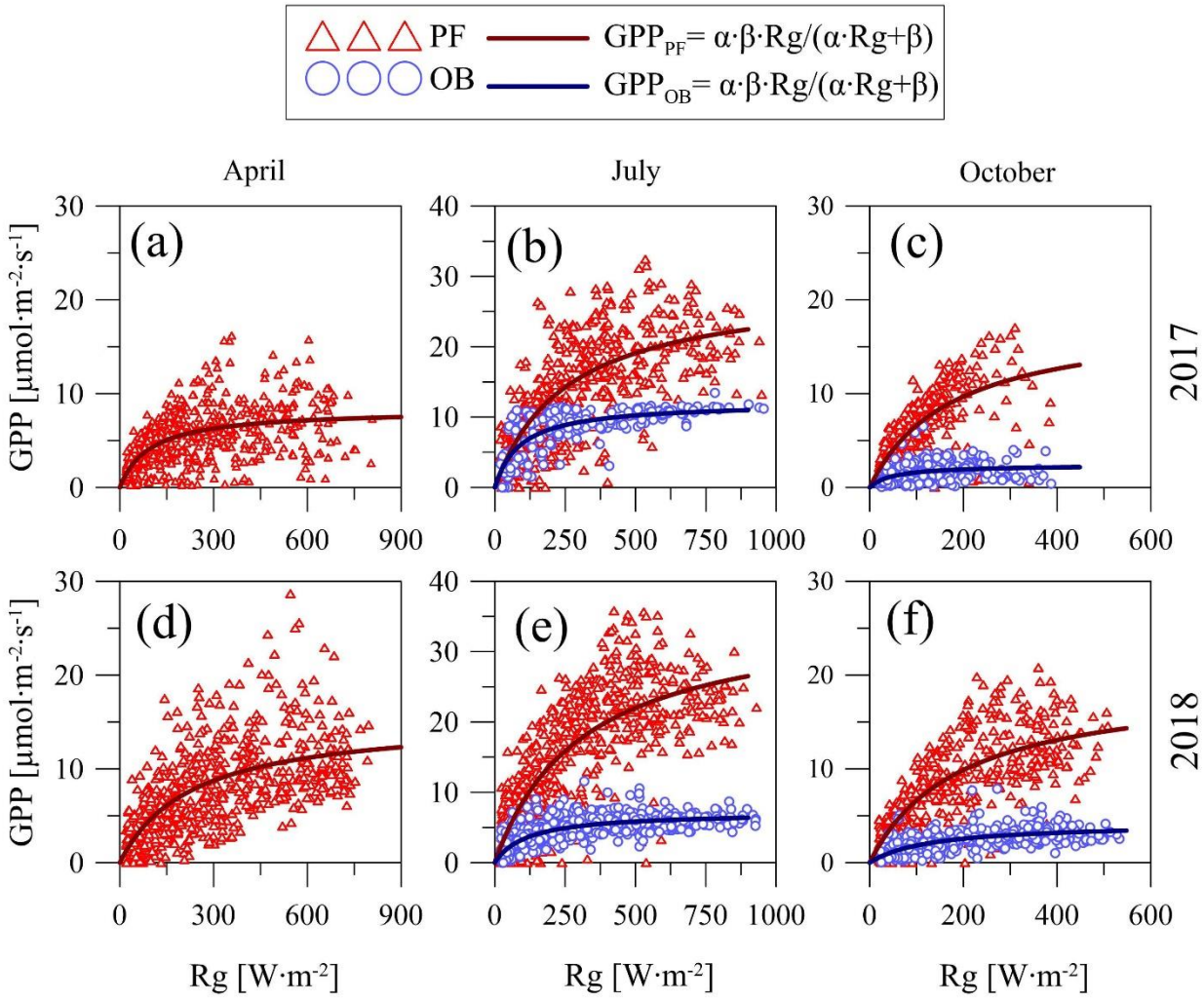

Figure 6. Hyperbolic light response curves (Eq. 3) of gross primary production (GPP) for April (a, d), July (b, e) and October (c, f) in 2017 and 2018 at paludified forest (PF) and ombrotrophic bog (OB) sites.

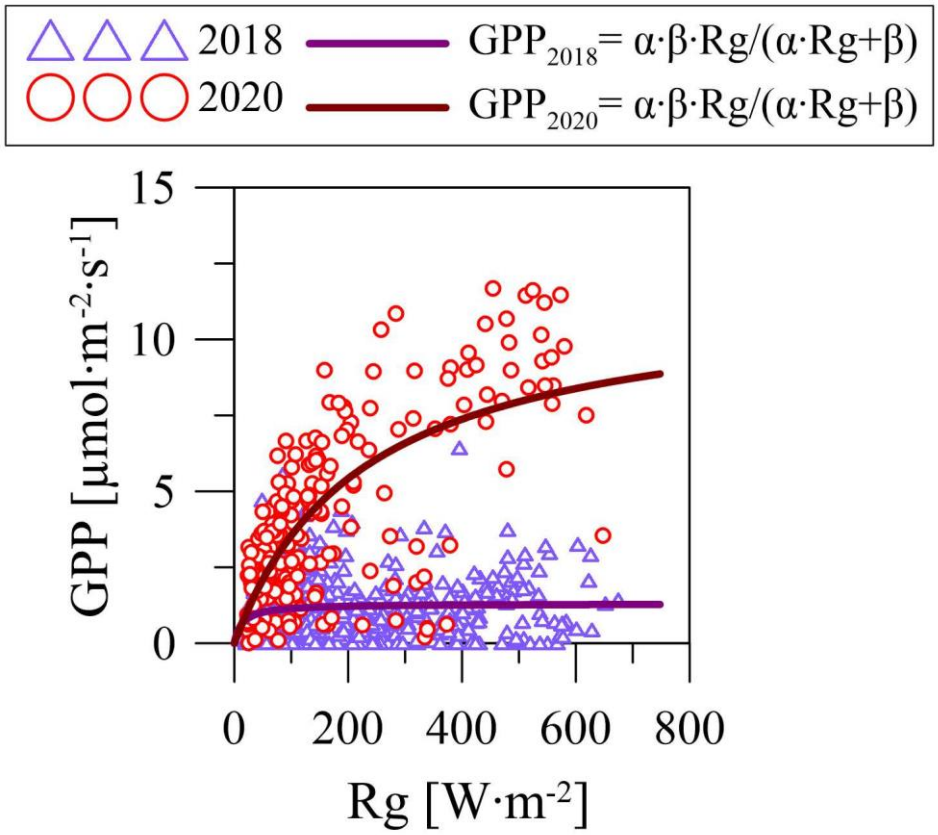

Figure 7 Hyperbolic light response curves (Eq. 3) of gross primary production (GPP) for March 2018 and 2020 at the paludified forest (PF).

420

Table 6. Parameters α and β of the light response curves (Eq. 3) and R^2 ($p<0.01$) for March, April, July and October in 2017, 2018 and 2020 at the paludified forest (PF) and the ombrotrophic bog (OB).

	α [µmol·J^{-1}]		**β [µmol·m^{-2}·s^{-1}]**		**R^2**	
	PF	**OB**	**PF**	**OB**	**PF**	**OB**
2017						
April	0.085	-	8.3	-	0.299	-
July	0.112	0.132	28.9	12.1	0.567	0.562
October	0.104	0.048	18.2	2.4	0.542	0.134
2018						

March	0.093	-	1.3	-	0.014	-
April	0.067	-	15.5	-	0.403	-
July	0.114	0.062	35.7	7.2	0.604	0.585
October	0.101	0.032	19.3	4.2	0.610	0.014
2020						
March	0.05	-	11.5	-	0.485	-

4. Discussion

4.1 Ecosystem CO_2 fluxes

Six years of paired eddy covariance measurements (2015-2020) at PF and OB sites showed that ombrotrophic bog in southern taiga of West Russia was a stronger CO_2 sink in the growing season than the adjacent paludified spruce forest excepting the warmest year of the period, however paludified spruce forest had a greater annual, growing season and daily TER and GPP than the adjacent bog. Therefore under the described environmental conditions the difference in annual and growing season CO_2 uptake of the ecosystems was dependent mostly on specific GPP/TER ratio rather than on difference in GPP. The growing season GPP/TER ratio at PF site was 0.98-1.12 and 1.32-1.40 at OB site and the annual value changed between 0.85 and 1.04 at PF site and was 1.23 at OB site in 2020. Annual and growing season values of GPP/TER ratio at PF site corresponded to the values obtained in old spruce forest on mineral soils located in 2 km to south from PF site (0.98) (Mamkin et al., 2019) and for black spruce (*Picea mariana*) stands on peaty soils reported by Dunn et al., (2007) in Manitoba (Canada) (annual: 0.89-1.09); Ueyama et al. (2014) (annual: 0.85-1.41 and the growing season: 0.90-1.61) and Euskirchen et al. (2014) (annual was about 1.04 and the growing season 1.14-1.47 with annual GPP/TER ratio for adjacent bog site about 1.08 and 1.30-1.42 in the growing season) on permafrost in Alaska (USA). GPP/TER ratio for OB site is also in agreement with the growing season values reported by Sulman et al. (2010) for bogs in Wisconsin (USA) (1.03) and Ontario (Canada) (1.30) but it was lower than GPP/TER ratio for bog in West Siberia (2.29) obtained by Alekseychik et al. (2017) in May-August period.

In spite of a numerous experiments focused on CO_2 fluxes at boreal and temperate peatlands (e.g. Martikainen et al., 1995; Lafleur et al., 2001; Aurela et al., 2002; Lindroth et al., 2007; Petrescu et al., 2015) it is a small number of studies based on simultaneous flux measurements at spruce forests and bogs located in the same landscape and undergo the similar weather conditions. The estimates of NEE at OB and PF sites (Table 3 and Table 4) are similar to the annual NEE obtained by Euskirchen et al., (2014) at permafrost in Alaska (USA) during the 3 years of measurements (between -76 and 72 $gC \cdot m^{-2} \cdot yr^{-1}$ at black spruce forest and between -81 and 23 $gC \cdot m^{-2} \cdot yr^{-1}$ at the bog) as well as TER and GPP sums at OB site (465-519 $gC \cdot m^{-2} \cdot yr^{-1}$ and 496-548 $gC \cdot m^{-2} \cdot yr^{-1}$ for TER and GPP respectively) while annual TER and GPP at black spruce forest was significantly lower than at PF site (491-633 $gC \cdot m^{-2} \cdot yr^{-1}$ and 544-588 $gC \cdot m^{-2} \cdot yr^{-1}$ for TER and GPP respectively). The similar annual and growing season NEE and larger TER and GPP sums at PF site in comparing with data from other black spruce stands was also detected. For example Ueyama et al., (2014) reported that growing season (April – September) sums of TER and GPP at the black spruce stand on permafrost in Alaska varied between 403-759 $gC \cdot m^{-2}$ and 491-799 $gC \cdot m^{-2}$ respectively and corresponding NEE values changed from -93 to 15 $gC \cdot m^{-2}$ during the 9 years of measurements, so the black spruce stand was primarily a sink of atmospheric CO_2. Dunn et al. (2007) also examined CO_2 fluxes in old black spruce forest in Manitoba (Canada) during the 9 years and found that annual NEE was -8 and 54 $gC \cdot m^{-2}$ with annual TER 611-826 $gC \cdot m^{-2} \cdot yr^{-1}$ and GPP 610-782 $gC \cdot m^{-2} \cdot yr^{-1}$. NEE as well as TER and GPP at PF site was, also similar to the estimates for the adjacent old spruce forest on mineral soils: NEE from April to mid-October 2016 was 24 $gC \cdot m^{-2}$ with corresponding TER =1373 $gC \cdot m^{-2}$ and GPP =1349 $gC \cdot m^{-2}$ (Mamkin et al., 2019). The relatively warm and wet weather conditions with long growing season and nutrient availability in southern taiga of Valdai Hills provide a favorable conditions for photosynthesis and ecosystem respiration of the boreal forests (Karpov, 1983) but its annual CO_2 uptake under the environmental conditions close to the long-term means is similar to the estimates from the other boreal forests located in colder climate and moreover is lower than the annual uptake at the bogs of the same landscape.

Larger CO_2 uptake at the Siberian spruce (*Picea obovata* Ledeb.) forest on peaty soils than at mesotrophic peatland located in 40 km from the forest in Nothern Ural (Komi republic, Russia) in April-August period was measured by Zagirova et al. (2019): NEE at the forest was -327 $gC \cdot m^{-2}$ and -140 $gC \cdot m^{-2}$ at the

mesotrophic peatland. NEE as well as TER and GPP sums for OB site is also corresponded to the estimates from other studies: For example NEE of the bog in Western Siberia in the period May-August as estimated by Alekseychik et al. (2017) was -202 $gC \cdot m^{-2}$ with corresponded TER and GPP values 157 $gC \cdot m^{-2}$ and 359 $gC \cdot m^{-2}$ respectively. Annual NEE at the bog in southern Sweden reported by Lund et al. (2007) was -21.5 $gC \cdot m^{-2}$.

Interannual variability and the long-term trends in environmental conditions could substantially influence annual NEE at southern taiga peatlands. The NEE estimated at PF site in 2015-2020 period (Table 3) was lower than NEE reported by Kurbatova et al. (2008) and measured at the same site in 1999 – 2004 period (100-600 $gC \cdot m^{-2} \cdot yr^{-1}$). The difference could be explained by positive air temperature trend in the last 20 years that enhanced GPP at the site and increasing in annual precipitation which therefore provided decreasing in WTD and consequently inhibited TER. The increasing of the CO_2 uptake at PF site due to the lowering in WTD is in agreement with model experiments carried out by Kurbatova et al. (2008).

Interannual variation of the growing season NEE at PF and OB sites as well as interannual variation of annual NEE in 2015-2020 is explained by changes in both TER and GPP rates and the maximal GPP values were observed in the years with increased Rg. Previous study at PF and OB sites (Kurbatova et al., 2013) demonstrated that TER play a key role in the NEE of the sites, especially in the relatively warm years. It is correspondent with (Dunn et al., 2007; Ueyama et al., 2014; Euskirchen et al., 2014) who showed that interannual changes in annual NEE of the black spruce stands in Alaska (USA) and Manitoba (Canada) was primarily dependent on TER variability than on changes in GPP. Strong dependence of NEE on TER was also obtained for fen in Alberta (Canada) by Cai et al. (2010).

It is considered, that relatively warm and dry weather conditions usually increase TER rates at the peatlands due to the enhanced soil and air temperature as well as WTD and can shift a peatland from CO_2 sink to CO_2 source (Moore, 2002; Drösler et al., 2008; Minkinnen et al., 2018). Thus, the drought events can be the major environmental factor of interannual variations of NEE at the peatlands controlling the TER rates (Welp et al.,2007; Lund et al., 2012). It is consistent with chamber measurements at OB site performed in the previous years and including an extreme drought 2010 in West Russia (Ivanov et al., 2017; Kurbatova et al., 2013). It is important to note that respiration rates measured by chambers and reported by Kurbatova et al. (2013) reached the maximum values and were more sensitive to temperature

variations under the weather conditions close to the long-term means in summer. Under the low WTD in the snowmelting period of spring and in extreme drought 2010 (with WTD>35 cm) respiration rates were lower and less sensitive to the temperature variations. In the period 2015-2020 there wasn't such extreme droughts and relatively low WTD variation was observed at OB site. At PF site a substantial increasing of WTD was detected in the growing seasons with the negative precipitation anomaly. In spite of the increased annual and growing season TER were detected in the years with high WTD the dependence of the 30-min and mean night-time TER on WTD was not found as well as at OB site. Therefore, the air and soil temperatures were the main predictors of seasonal variations of TER at the sites in the selected years. Weak dependence of TER and NEE to WTD at the peatlands was reported in many studies (e.g. Lafleur et al., 2001; Lafleur et al., 2005; Parmentier et al., 2009; Sulman et al., 2009; Alekseychik et al., 2017). For example, Parmentier et al. (2009) hypothesized that increasing in WTD will affect TER on peatland if WTD changes are accompanied by changes in soil water content. Lafleur et al. (2005) suggested that dependence of TER on WTD is a result of complex interactions between WTD, vertical profiles of peat water content in the unsaturated zone above the water table, and vertical profiles of peat decomposability and supposed that TER at wetter peatlands should be more sensitive to changes in WTD. Sulman et al., (2009) detected that lowering in water level increase both TER and GPP and lead to small dependence of NEE on the peatland to changes in WTD. It is feasible that small changes in WTD and uniform distribution of precipitation during the study period preserved the peat layer properties at PF and OB sites and the strong dependence of TER and NEE on WTD would be detectable if droughts would be more frequent in the region.

The sensitivity parameters of TER (Q_{10}) to soil and air temperatures (Table 5 and Table 6) corresponded to the values obtained in the other studies (Lafleur et al., 2005; Humphreys et al., 2006; Lindroth et al., 2007; Lund et al., 2007; Ueyama et al., 2014). For example Humphreys et al. (2006) obtained mid-summer Q_{10} values calculated using air temperature for bog and different fens in Canada between 1.3 – 2.0 and R_{10} was 0.9 – 3.2 $\mu mol \cdot m^{-2} \cdot s^{-1}$. Lund et al. (2007) reported that Q_{10} at the temperate bog in Sweden was 1.81 when air temperature was used for calculation and 2.83 was obtained using soil temperature at 5 cm depth. Also, a slightly different Q_{10} were obtained depending on microtopography of the bog: corresponding Q_{10} values for hummocks were 2.32 and 2.54 for hollows. Lafleur et al. (2005)

estimated Q_{10} values at the bog in Ontario (Canada): 2.24 when air temperature at 50 cm height was used, 2.57 at hummock and 3.91 at hollow. Q_{10} at the black spruce stand in Alaska (USA) in the growing season reported by Ueyama et al. (2014) and calculated using air temperature ranged between 1.5-2.5. However Q_{10} values calculated for PF site were lower than for adjacent spruce forest on mineral soils in the growing season 2016: 2.49 and 5.77 calculated using air and soil temperature respectively and reported by Mamkin et al. (2019). The corresponded R_{10} values were 5.43 and 5.77 respectively. Lower sensitivity of TER on PF and OB sites in comparing with the adjacent forest on mineral soils could be connected with both decreased heterotrophic and autotrophic respiration due to the paludification which inhibits decomposition processes in the upper soil layers and limit productivity of the ecosystems.

4.2 Uncertainty of the seasonal and annual ecosystem CO_2 fluxes.

Uncertainty associated with random error in the measured fluxes and data processing was about 2-8% of the annual and growing season TER and GPP at the sites and exceeded annual and growing season NEE in several years at PF site. Considering the uncertainty of the CO_2 flux estimates it is difficult to identify the current status of PF as atmospheric CO_2 source or sink straightforward. It is likely that annual NEE at PF site is close to 0 but in most of the growing seasons of the period it was a sink. Unlike PF site, OB site had lower NEE uncertainty than the growing season and annual (in 2020) net CO_2 uptake rates, hence OB site is functioning as a CO_2 sink for the atmosphere. Although an increase of the CO_2 sequestration by PF site and GPP/TER ratio was observed in the warmest 2020 year as well as decreased TER and GPP values in the coldest 2017 year it is challenging to attribute interannual changes in CO_2 fluxes with the environmental conditions in other years due to the range of uncertainty similar to the interannual flux variability.

4.3 Implications of climate change in the region for peatlands.

Observed warming trend in the boreal ecozone lead to the increasing in both TER and GPP (Aurela et al., 2004; Minkkinen et al., 2018; IPCC, 2019). But the net effect on NEE (shifting ecosystem status to CO_2 source or CO_2 sink for the atmosphere) can vary across the ecosystems depending on local environmental conditions, hydrology and vegetation type. The six years of eddy covariance measurements at PF and OB

sites showed that positive temperature anomaly can increase proportion of the winter fluxes to the annual sums. At PF site positive anomaly in winter months mainly increase production and decomposition processes (mainly GPP) while at OB site changes of TER and GPP are not significant. Winter NEE in boreal peatlands is usually depended on TER rates (Fahnestock et al., 1999; Koehler et al., 2010; Lohila et al., 2011). The growth of winter air and soil temperature can potentially increase CO_2 release. Several studies showed that winter emission in boreal peatlands can offset the summer CO_2 uptake (Alm et al., 1999; Lafleur et al., 2001; D'Acunha et al., 2019).

Previous studies carried out at the same sites using eddy covariance and chamber measurements as well as modelling experiments (Miliukova et al., 2002; Kurbatova et al., 2008; Kurbatova et al., 2013) suggested that climate warming can increase TER and consequently NEE of the bogs and paludified forests in the region. In this study we estimated that interannual variability of GPP driven by temperature anomaly can substantially influence annual and seasonal NEE of the selected ecosystems and positive temperature anomaly lead to the increasing of the CO_2 uptake of the paludified forest. It is corresponded with Dunn et al. (2007) who showed that black spruce forest on peaty soils in Manitoba (Canada) switched from CO_2 source to CO_2 sink in several years following the positive temperature trend. The different response of NEE on positive temperature anomaly in previous studies and in the present research is likely connected with difference in moisture regime at PF and OB sites between 1999-2011 and 2015-2020 periods. So under the hot and dry conditions the ecosystems were a CO_2 source for the atmosphere which is in agreement with several studies at the similar ecosystems (Lund et al., 2007; Cai et al., 2010). It is likely that increasing in precipitation during the last decades which was uniformly distributed over a growing season period provided a low WTD and created a favourable conditions for growing in GPP and increasing of the CO_2 uptake at the sites.

Influence of present warming trend on NEE of the peatlands is also dependent on the season when the substantial changes in air temperature and precipitation are observed. Shifting of the growing season start and snowmelting period can additionally impact the annual NEE. For example, late snowmelting and the late start of the growing season followed by a hot and dry summer in Alaska (USA) switched black spruce permafrost forest and adjacent bog from CO_2 sink (under temperature and precipitation close to the long-term means) to the CO_2 source for the atmosphere (Euskirchen et al., 2014). Conversely, early start of the

growing season and snowmelting can lead to the increasing in annual CO_2 uptake and therefore the environmental conditions in spring can determine the annual CO_2 balance of the forest and bog ecosystems that was reported in many experimental studies (Lafleur et al., 2001; Aurela et al., 2004; Syed et al., 2006; Black et al., 2000; Hommeltenberg et al., 2014). However, the research provided by Goulden et al. (1998) showed that a positive air temperature trend in spring can lead to the substantial carbon loss in an old black spruce forest in Manitoba (Canada). An important factor of the spring NEE can be a thaw water supply. For example Hu et al. (2010) reported that early seasonal warming with lack of thaw water in spring decreased CO_2 uptake of subalpine pine-aspen forest in Colorado Rocky Mountains (USA).

The response of CO_2 fluxes at PF and OB sites on positive temperature anomaly in spring was different. CO_2 uptake at paludified spruce forest began before the snowmelting and the anomalously warm conditions in late winter and early spring provided a substantial increasing in GPP while the CO_2 uptake at the bog observed after the start of the growing season. Thus, we expect that increased frequency of thaw weather periods in winter that was predicted in West Russia (Roshydromet, 2014; IPCC, 2014) and early spring can increase CO_2 uptake of the paludified forest with less significant changes of NEE at the bog. Unlike warm springs, warm autumn can increase TER more than GPP and consequently reduce an annual CO_2 sequestration (Piao et al., 2008; Ueyama et al., 2014).

According to the meteorological observations during the last 30 years mean annual air temperature and annual precipitation on Valdai hills show a positive trends in the last decades which is mostly connected with increasing in winter temperature and precipitation however the thickness of snowpack and the period with snow cover is decreasing. Moreover, the growing season became longer primarily due to the shifting of the start of the growing season to early dates in spring with no significant shift of the end of the growing season in autumn. According to the current climate changes an increasing of CO_2 sequestration at peatlands due to the enhanced GPP rates, especially at forest ecosystems, in early spring in the west part of Valdai Hills is expectable. However, the latest climate predictions (IPCC, 2021) for the region showed that future warming in the next decades will be attended with increasing in winter precipitation and decreasing in summer. Thus in spite of the positive trend in annual precipitation a raising frequency of heat waves and droughts in summer is also presumable. While warming and moistening in winter could increase GPP more than TER especially at paludified forests, the extreme hot and dry conditions are able

to increase heterotrophic respiration significantly and switch peatlands from CO_2 sink to a consistent CO_2 source for the atmosphere as well as alter NPP of the ecosystems. For example, SPRUCE experiment in Minnesota (USA) showed a significant carbon loss rates at black spruce stands on the bog (higher than its historical accumulation rates) under the warming treatment which was connected with increased heterotrophic respiration, decreased *Sphagnum* and tree above ground NPP (Walker et al., 2017; Hanson et al., 2020).

Noting that: PF site is charachterized by high interannual variability of NEE which is close to 0 and a relatively high daily, growing season and annual TER and GPP as well as high sensitivity of TER and GPP to the changes in environmental factors, the observed warming trend can affect the status of the paludified forests in southern taiga as a source or sink of atmospheric CO_2 more than bogs located in the same landscape. Therefore, we can expect an increasing role of the moistening conditions under future climate change for the ecosystem status as a source or sink of atmospheric CO_2 in southern taiga of West Russia.

Conclusions

Six years of paired eddy covariance CO_2 flux measurements at paludified spruce forest and adjacent ombrotrophic bog in southern taiga of west Russia during 2015-2020 period showed that PF site had a higher daily, growing season and annual TER and GPP rates as well as its sensitivity to the environmental variables than at OB site. OB site was a sink of atmospheric CO_2 (NEE<0) in the growing seasons with higher GPP/TER ratios while PF was a CO_2 source or sink with annual and growing season NEE close to zero. Considering the high variability of TER and GPP rates, PF can be a stronger CO_2 sink than OB site in the particular years (e.g. in 2020). Positive temperature anomaly in winter 2019/2020 lead to the increased daily GPP and TER values as well as GPP/TER ratio at PF site in non-growing season, especially in early spring. At OB site the changes in TER, GPP and NEE between the relatively cold and warm winters were not significant. The increased daily GPP/TER ratio in the warmest and the wettest year of the period (2020) at PF site was detected. Therefore, the positive temperature anomaly in late winter and early spring can potentially increase CO_2 uptake of the southern taiga paludified spruce forests more than of the bogs in the same landscapes. However, if the drought events associated with the expected

climate change will be more frequent in the region the increasing in TER rates can overlap the effect of increasing GPP rates and switch the paludified forest to a consistent CO_2 source for the atmosphere. We also expect the increasing role of the moistening conditions in the regulating the future status of the southern taiga peatlands as a carbon dioxide source or sink under the warming trend.

Data availability

The data used in this publication will be provided upon request. The eddy covariance and meteorological data obtained at PF site are available at European Fluxes Database Cluster database (http://www.europe-fluxdata.eu/).

Author contribution

VM designed the study, performed the data analysis as well as field measurements at PF site and wrote the major part of the text. VA designed and performed the field measurements at OB site. DI performed the field measurements and data processing. AV designed the study and field measurements at PF site. JK designed the study and wrote the text.

Competing interests

The authors declare that they have no conflict of interest.

Aknowledgements

This study was supported by the grants of the Russian Science Foundation (21-14-00209) and the Russian Foundation for Basic Research (project 19-04-01234-a). The flux data processing and data analysis performed by Mamkin V., Ivanov D., Varlagin A. and Kurbatova J. were supported by the grant of the Russian Science Foundation (21-14-00209). The field measurements provided by Mamkin V. and Varlagin A. was supported by the grant of the Russian Foundation for Basic Research (project 19-04-01234-a).

References

Alekseychik, P., Mammarella, I., Karpov, D., Dengel, S., Terentieva, I., Sabrekov, A., Glagolev M. and Lapshina, E.: Net ecosystem exchange and energy fluxes measured with the eddy covariance

technique in a western Siberian bog. Atmos chem phys, 17(15), 9333-9345,doi: 10.5194/acp-2021-641 , 2017.

Alexandrov, G. A., Brovkin, V. A., Kleinen, T., and Yu, Z.: The capacity of northern peatlands for long-term carbon sequestration, Biogeosciences, 17, 47–54, doi: 10.5194/bg-17-47-2020, 2020.

Alm, J., Schulman, L., Walden, J., Nykänen, H., Martikainen, P. J. and Silvola, J.: Carbon balance of a boreal bog during a year with an exceptionally dry summer, Ecology, 80(1), 161-174, doi: 10.1890/0012-9658(1999)080[0161:CBOABB]2.0.CO;2, 1999.

Aurela, M., Laurila, T. and Tuovinen, J. P.: Annual CO_2 balance of a subarctic fen in northern Europe: Importance of the wintertime efflux, J Geophys Res-Atmos, 107(D21), ACH 17-1-ACH 17-12, doi: 10.1029/2002JD002055, 2002.

Aurela, M., Laurila, T. and Tuovinen, J. P.: The timing of snow melt controls the annual CO_2 balance in a subarctic fen, Geophys Res Lett, 31(16), doi: 10.1029/2004GL020315, 2004.

Beaulne, J., Garneau, M., Magnan, G. and Boucher, É.: Peat deposits store more carbon than trees in forested peatlands of the boreal biome, Sci Rep-UK, 11(1), 1-11, doi: 10.1038/s41598-021-82004-x, 2021.

Black, T. A., Chen, W. J., Barr, A. G., Arain, M. A., Chen, Z., Nesic, Z., Hogg, E.H., Neumann H.H., Yang, P. C.: Increased carbon sequestration by a boreal deciduous forest in years with a warm spring, Geophys Res Lett, 27(9), 1271-1274, doi: 10.1029/1999GL011234, 2000.

Buitenwerf, R., Rose, L. and Higgins S.I.: Three decades of multi-dimensional change in global leaf phenology, Nat Clim Change, 5, 364-368, doi: 10.1038/nclimate2533, 2015.

Cai, T., Flanagan, L. B. and Syed, K. H.: Warmer and drier conditions stimulate respiration more than photosynthesis in a boreal peatland ecosystem: analysis of automatic chambers and eddy covariance measurements, Plant, cell and environ, 33(3), 394-407, doi: 10.1111/j.1365-3040.2009.02089.x, 2010.

D′ Acunha, B., Morillas, L., Black, T. A., Christen, A. and Johnson, M. S.: Net ecosystem carbon balance of a peat bog undergoing restoration: integrating CO_2 and CH_4 fluxes from eddy covariance and aquatic evasion with DOC drainage fluxes, J Geophys Res-Biogeo, 124(4), 884-901, doi: 10.1029/2019JG005123, 2019.

Desherevskaya, O., Kurbatova, J. and Olchev, A.: Climatic conditions of the south part of Valday Hills, Russia, and their projected changes during the 21st century, The Open Geography Journal, 3, 73-79, doi: 10.2174/1874923201003010073, 2010.

Dunn, A. L., Barford, C. C., Wofsy, S. C., Goulden, M. L. and Daube, B. C.: A long-term record of carbon exchange in a boreal black spruce forest: Means, responses to interannual variability, and decadal trends, Glob Change Biol, 13(3), 577-590, doi: 10.1111/j.1365-2486.2006.01221.x, 2007.

Donat, M.G., Alexander, L. V., Yang, H., Durre, I., Vose, R., Dunn, R. J. H., Willett, K. M., Aguilar, E., Brunet, M., Caesar, J., Hewitson, B., Jack, C., Klein Tank, A. M. G., Kruger, A. C., Marengo, J., Peterson, T. C., Renom, M., Oria Rojas, C., Rusticucci, M., Salinger, J., Elrayah, A. S., Sekele, S. S., Srivastava, A. K., Trewin, B., Villarroel, C., Vincent, L. A., Zhai, P., Zhang, X. and Kitching S.: Updated analyses of temperature and precipitation extreme indices since the beginning of the twentieth century: The HadEX2 dataset, J Geophys Res-Atmos 118, 2098–2118, doi: 10.1002/jgrd.50150, 2013.

Drösler, M., Freibauer, A., Christensen, T. R. and Friborg, T.: Observations and status of peatland greenhouse gas emissions in Europe, in: The Continental-Scale Greenhouse Gas Balance of Europe. Ecological Studies., edited by Dolman, A.J., Valentini, R., Freibauer, A., Springer, New York, USA, 243-261, doi: 10.1007/978-0-387-76570-9_12, 2008.

Euskirchen, E. S., Edgar, C. W., Turetsky, M. R., Waldrop, M. P. and Harden, J. W.: Differential response of carbon fluxes to climate in three peatland ecosystems that vary in the presence and stability of permafrost, J Geophys Res-Biogeo, 119(8), 1576-1595, doi: 10.1002/2014JG002683, 2014.

Fahnestock, J. T., Jones, M. H. and Welker, J. M.: Wintertime CO_2 efflux from arctic soils: implications for annual carbon budgets, Global Biogeochem Cy, 13(3), 775-779, doi: doi.org/10.1029/1999GB900006, 1999.

Friedlingstein, P., Jones, M. W., O'Sullivan, M., Andrew, R. M., Hauck, J., Peters, G. P., Peters, W., Pongratz, J., Sitch, S., Le Quéré, C., Bakker, D. C. E., Canadell, J. G., Ciais, P., Jackson, R. B., Anthoni, P., Barbero, L., Bastos, A., Bastrikov, V., Becker, M., Bopp, L., Buitenhuis, E., Chandra, N., Chevallier, F., Chini, L. P., Currie, K. I., Feely, R. A., Gehlen, M., Gilfillan, D., Gkritzalis, T.,

Goll, D. S., Gruber, N., Gutekunst, S., Harris, I., Haverd, V., Houghton, R. A., Hurtt, G., Ilyina, T., Jain, A. K., Joetzjer, E., Kaplan, J. O., Kato, E., Klein Goldewijk, K., Korsbakken, J. I., Landschützer, P., Lauvset, S. K., Lefèvre, N., Lenton, A., Lienert, S., Lombardozzi, D., Marland, G., McGuire, P. C., Melton, J. R., Metzl, N., Munro, D. R., Nabel, J. E. M. S., Nakaoka, S.-I., Neill, C., Omar, A. M., Ono, T., Peregon, A., Pierrot, D., Poulter, B., Rehder, G., Resplandy, L., Robertson, E., Rödenbeck, C., Séférian, R., Schwinger, J., Smith, N., Tans, P. P., Tian, H., Tilbrook, B., Tubiello, F. N., van der Werf, G. R., Wiltshire, A. J., and Zaehle, S.: Global Carbon Budget 2019, Earth Syst. Sci. Data, 11, 1783–1838, doi: 10.5194/essd-11-1783-2019, 2019.

Gill, A. L., Giasson, M. A., Yu, R. and Finzi, A. C.: Deep peat warming increases surface methane and carbon dioxide emissions in a black spruce-dominated ombrotrophic bog, Glob Change Biol, 23(12), 5398-5411, doi: 10.1111/gcb.13806, 2017.

Gorham, E.: Northern peatlands: role in the carbon cycle and probable responses to climatic warming, Ecol appl, 1(2), 182-195, doi: 10.2307/1941811, 1991.

Goulden, M. L., Wofsy, S. C., Harden, J. W., Trumbore, S. E., Crill, P. M., Gower, S. T., Fries, T., Daube, B. C., Fand, S.-M., Sutton, J., Bazzaz, A. and Munger, J. W.: Sensitivity of boreal forest carbon balance to soil thaw, Science, 279(5348), 214-217, doi: 10.1126/science.279.5348.214, 1998.

Greco, S. and Baldocchi, D. D.: Seasonal variations of CO_2 and water vapour exchange rates over a temperate deciduous forest. Glob Change Biol, 2(3), 183-197, doi: 10.1111/j.1365-2486.1996.tb00071.x, 1996.

Hanson, P. J., Griffiths, N. A., Iversen, C. M., Norby, R. J., Sebestyen, S. D., Phillips, J. R., Chanton, J.P., Kolka, R.K., Malhotra, A., Oleheiser, K. C., Warren, J.M., Shi, X., Yang, X., Mao, J., Ricciuto, D. M.: Rapid net carbon loss from a whole-ecosystem warmed Peatland. AGU Advances, 1(3), e2020AV000163, doi: 10.1029/2020AV000163, 2020.

Helbig, M., Chasmer, L. E., Desai, A. R., Kljun, N., Quinton, W. L., Sonnentag, O.: Direct and indirect climate change effects on carbon dioxide fluxes in a thawing boreal forest-wetland landscape. Glob Change Biol, 23(8), 3231–3248, doi:10.1111/gcb.13638, 2017.

Helbig, M., Humphreys, E. R., Todd, A.: Contrasting temperature sensitivity of CO_2 exchange in peatlands of the Hudson Bay Lowlands, Canada. Journal of Geophysical Research: Biogeosciences, 124(7), 2126-2143, 2019.

Helbig, M., Waddington, J. M., Alekseychik, P., Amiro, B., Aurela, M., Barr, A. G., Black, T.A., Carey, S.K., Chen, J., Chi, J., Desai, A.R., Dunn, A., Euskirchen, E.S., Flanagan, L.B., Friborg, T., Garneau, M., Grelle, A., Harder, S., Heliasz, M., Humphreys, E.R., Ikawa, H., Isabelle, P.-E., Iwata, H., Jassal, R., Korkiakoski M., Kurbatova, J, Kutzbach, L., Lapshina, E., Lindroth, A., Ottosson Löfvenius, M., Lohila, A., Mammarella, I., Marsh, P., Moore, P.A., Maximov, T., Nadeau, D.F., Nicholls, E.M., Nilsson, M.B., Ohta, T., Peich, M., Petrone, R.M., Prokushkin, A., Quinton, W.L., Roulet, N.,19, Runkle, B.R.K., Sonnentag, O., Strachan, I.B., Taillardat, P., Tuittila, E.-S., Tuovinen, J.-K., Turner, J., Ueyama, M., Varlagin, A., Vesala, T., Wilmking, M., Zyrianov, V. and Schulze, C.: The biophysical climate mitigation potential of boreal peatlands during the growing season, Environ Res Lett, 15(10), 104004. doi: 10.1088/1748-9326/abab34, 2020.

Holl, D., Pfeiffer, E.-M., and Kutzbach, L.: Comparison of eddy covariance CO2 and CH4 fluxes from mined and recently rewetted sections in a northwestern German cutover bog, Biogeosciences, 17, 2853–2874, doi: 10.5194/bg-17-2853-2020, 2020.

Hommeltenberg, J., Schmid, H. P., Drösler, M., and Werle, P.: Can a bog drained for forestry be a stronger carbon sink than a natural bog forest?, Biogeosciences, 11, 3477–3493, doi: 10.5194/bg-11-3477-2014, 2014.

Hu, J. I. A., Moore, D. J., Burns, S. P. and Monson, R. K.: Longer growing seasons lead to less carbon sequestration by a subalpine forest, Glob Change Biol, 16(2), 771-783, doi: 10.1111/j.1365-2486.2009.01967.x, 2010.

Humphreys, E. R., Lafleur, P. M., Flanagan, L. B., Hedstrom, N., Syed, K. H., Glenn, A. J. and Granger, R.: Summer carbon dioxide and water vapor fluxes across a range of northern peatlands. J Geophys Res-Biogeo, 111(G4), doi: 10.1029/2005JG000111, 2006.

IPCC: Climate Change 2014: Synthesis Report. Contribution of Working Groups I, II and III to the Fifth Assessment Report of the Intergovernmental Panel on Climate Change [Core Writing Team, R.K. Pachauri and L.A. Meyer (eds.)], IPCC, Geneva, Switzerland, 151 pp., 2014.

IPCC: C. C. Land: An IPCC Special Report on Climate Change, Desertification, Land Degradation, Sustainable Land Management, Food Security, and Greenhouse Gas Fluxes In Terrestrial Ecosystems. Intergovernmental Panel on Climate Change, 1542 pp., 2019.

IPCC: Climate Change 2021. The Physical Science Basis. Contribution of Working Group I to the Sixth Assessment Report of the Intergovernmental Panel on Climate Change [Masson-Delmotte, V., P. Zhai, A. Pirani, S.L. Connors, C. Péan, S. Berger, N. Caud, Y. Chen, L. Goldfarb, M.I. Gomis, M. Huang, K. Leitzell, E. Lonnoy, J.B.R., Matthews, T.K. Maycock, T. Waterfield, O. Yelekçi, R. Yu, and B. Zhou (eds.)]. Cambridge University Press. In Press, 2021.

Ivanov, D. G., Avilov, V. K., Kurbatova, Y. A.: CO_2 fluxes at south taiga bog in the European part of Russia in summer. Contemporary Problems of Ecology, 10(2), 97-104, doi: 10.1134/S1995425517020056, 2017.

Ivanov, D. G., Kotlov, I. P., Minayeva, T. Y. and Kurbatova, J. A. Estimation of carbon dioxide fluxes on a ridge-hollow bog complex using a high resolution orthophotoplan, Nature conservation research, 6(2), 16–28, doi: 10.24189/ncr.2021.020, 2021.

Karpov, V. G.: Spruce forests of the territory, in: Regulation of factors of spruce forest ecosystems, edited by: Karpov, V. G., Nauka, Leningrad, USSR, 7–31, 1983 (in Russian).

Kljun, N., Calanca, P., Rotach, M. W. and Schmid, H. P.: A simple parameterisation for flux footprint predictions, Boundary-Layer Meteorology, 112(3), 503-523, doi: 10.1023/B:BOUN.0000030653.71031.96, 2004.

Koehler, A. K., Sottocornola, M. and Kiely, G.: How strong is the current carbon sequestration of an Atlantic blanket bog?, Glob Change Biol, 17(1), 309-319, doi: 10.1111/j.1365-2486.2010.02180.x, 2011.

Kolle, O. and Rebmann, C.: EddySoft – Documentation of a Software Package to Aquire and Process Eddy Covariance Data, Max-Planck-Institut f¨ur Biogeochemie, Jena, Germany, Technical Report 10, 85 pp., 2007.

Kurbatova, J., Arneth, A., Vygodskaya, N. N., Kolle, O., Varlargin, A. V., Milyukova, I. M., Tchebakova, N.M., Schulze, E.-D. and Lloyd, J.: Comparative ecosystem–atmosphere exchange of energy and mass in a European Russian and a central Siberian bog I. Interseasonal and interannual

variability of energy and latent heat fluxes during the snowfree period. Tellus B, 54(5), 497-513, doi: 10.3402/tellusb.v54i5.16683, 2002.

Kurbatova, J., Li, C., Varlagin, A., Xiao, X., and Vygodskaya, N.: Modeling carbon dynamics in two adjacent spruce forests with different soil conditions in Russia, Biogeosciences, 5, 969–980, doi: 10.5194/bg-5-969-2008, 2008.

Kurbatova, J., Tatarinov, F., Molchanov, A., Varlagin, A., Avilov, V., Kozlov, D., Ivanov, D. and Valentini, R.: Partitioning of ecosystem respiration in a paludified shallow-peat spruce forest in the southern taiga of European Russia, Environ Res Lett, 8(4), 045028, doi: 10.1088/1748-9326/8/4/045028, 2013.

Kuricheva, O., Mamkin, V., Sandlersky, R., Puzachenko, J., Varlagin, A. and Kurbatova, J.: Radiative entropy production along the paludification gradient in the southern taiga, Entropy, 19(1), 43, doi: 10.3390/e19010043, 2017.

Lafleur, P. M., Griffis, T. J. and Rouse, W. R.: Interannual variability in net ecosystem CO_2 exchange at the arctic treeline, Arct Antarct Alp Res, 33(2), 149-157, doi: 10.1080/15230430.2001.12003417, 2001.

Lafleur, P. M., Moore, T. R., Roulet, N. T. and Frolking, S.: Ecosystem respiration in a cool temperate bog depends on peat temperature but not water table, Ecosystems, 8(6), 619-629, doi: 10.1007/s10021-003-0131-2, 2005.

Lafleur, B., Fenton, N. J. and Bergeron, Y.: Forecasting the development of boreal paludified forests in response to climate change: a case study using Ontario ecosite classification, Forest Ecosystems, 2(1), 1-11, doi: 10.1186/s40663-015-0027-6, 2015.

Lavoie, M., Paré, D. and Bergeron, Y. Impact of global change and forest management on carbon sequestration in northern forested peatlands, Environ Rev, 13(4), 199-240, doi: 10.1139/a05-014, 2005.

Lindroth, A., Lund, M., Nilsson, M., Aurela, M., Christensen, T. R., Laurila, T., Rinne, J., Riutta, T., Sagerfors, J., Ström, L., Tuovinen J.-P. and Vesala, T.: Environmental controls on the CO_2 exchange in north European mires. Tellus B, 59(5), 812-825, doi: 10.1111/j.1600-0889.2007.00310.x, 2007.

Loisel, J., Gallego-Sala, A. V., Amesbury, M. J., Magnan, G., Anshari, G., Beilman, D. W., Benavides, J. C., Blewett, J., Camill, P. , Charman, D. J., Chawchai, S., Hedgpeth, A., Kleinen, T., Korhola, A., Large, D., Mansilla, C. A., Müller, J., van Bellen, S., West, J. B., Yu, Z., Bubier, J. L., Garneau, M., Moore, T., Sannel, A. B. K., Page, S., Väliranta, M., Bechtold, M., Brovkin, V., Cole, L. E. S., Chanton, J. P., Christensen, T. R., Davies, M. A., De Vleeschouwer, F., Finkelstein, S. A., Frolking, S., Gałka, M., Gandois, L., Girkin, N., Harris, L. I., Heinemeyer, A., Hoyt, A. M., Jones, M. C., Joos, F., Juutinen, S., Kaiser, K., Lacourse, T., Lamentowicz, M., Larmola, T., Leifeld, J., Lohila, A., Milner, A. M., Minkkinen, K., Moss, P., Naafs, B. D. A., Nichols, J., O'Donnell, J., Payne, R., Philben, M., Piilo, S., Quillet, A., Ratnayake, A. S., Roland, T. P., Sjögersten, S., Sonnentag, O., Swindles, G. T., Swinnen, W., Talbot, J., Treat, C., Valach, A. C. and Wu, J.: Expert assessment of future vulnerability of the global peatland carbon sink, Nat Clim Change, 11(1), 70-77, doi: 10.1038/s41558-020-00944-0, 2021.

Lohila, A., Minkkinen, K., Aurela, M., Tuovinen, J.-P., Penttilä, T., Ojanen, P., and Laurila, T.: Greenhouse gas flux measurements in a forestry-drained peatland indicate a large carbon sink, Biogeosciences, 8, 3203–3218, doi:10.5194/bg-8-3203-2011, 2011.

Lund, M., Lindroth, A., Christensen, T. R. and Stroem, L.: Annual CO_2 balance of a temperate bog, Tellus B, 59(5), 804-811, doi: 10.1111/j.1600-0889.2007.00303.x, 2007.

Lund, M., Christensen, T. R., Lindroth, A. and Schubert, P.: Effects of drought conditions on the carbon dioxide dynamics in a temperate peatland, Environ Res Lett, 7(4), 045704, doi: 10.1088/1748-9326/7/4/045704, 2012.

Mamkin, V., Kurbatova, J., Avilov, V., Ivanov, D., Kuricheva, O., Varlagin, A., Yaseneva, I. and Olchev, A.: Energy and CO_2 exchange in an undisturbed spruce forest and clear-cut in the Southern Taiga, Agr forest meteorol, 265, 252-268., doi: 10.1016/j.agrformet.2018.11.018, 2019.

Martikainen, P. J., Nykänen, H., Alm, J. and Silvola, J.: Change in fluxes of carbon dioxide, methane and nitrous oxide due to forest drainage of mire sites of different trophy, Plant Soil, 168(1), 571-577, doi: 10.1007/BF00029370, 1995.

Milyukova, I. M., Kolle, O., Varlagin, A. V., Vygodskaya, N. N., Schulze, E. D. and Lloyd, J.: Carbon balance of a southern taiga spruce stand in European Russia, Tellus B, 54(5), 429-442, doi: 10.3402/tellusb.v54i5.16679, 2002.

Minkkinen, K., Ojanen, P., Penttilä, T., Aurela, M., Laurila, T., Tuovinen, J.-P., and Lohila, A.: Persistent carbon sink at a boreal drained bog forest, Biogeosciences, 15, 3603–3624, doi: 10.5194/bg-15-3603-2018, 2018.

Moore, P. D.: The future of cool temperate bogs, Environ conserv, 29(1), 3-20, doi: 10.1017/S0376892902000024, 2002.

Mueller, B., Hauser, M. Iles, C., Haque Rimi, R., Zwiers, F., W. and Wan, H.: Lengthening of the growing season in wheat and maize producing regions, Weather and Climate Extremes, 9, 47–56, doi: 10.1016/j.wace.2015.04.001, 2015.

Matthews, B., Mayer, M., Katzensteiner, K., Godbold, D. L. and Schume, H.: Turbulent energy and carbon dioxide exchange along an early-successional windthrow chronosequence in the European Alps, Agr for meteorol, 232, 576-594, doi: 10.1016/j.agrformet.2016.10.011, 2017.

Mauder, M. and Foken, T.: Impact of post-field data processing on eddy covariance flux estimates and energy balance closure, Meteorol Z, 15(6), 597-610, doi: 10.1127/0941-2948/2006/0167, 2006.

Mauder, M., Cuntz, M., Drüe, C., Graf, A., Rebmann, C., Schmid, H. P., Schmidt, M., Steinbrecher, R.: A strategy for quality and uncertainty assessment of long-term eddy-covariance measurements, Agr forest meteorol, 169, 122-135, doi: 10.1016/j.agrformet.2012.09.006, 2013.

Novenko, E. Y., Olchev, A. V.: Early Holocene vegetation and climate dynamics in the central part of the East European Plain (Russia), Quaternary International, 388, 12-22, doi: 10.1016/j.quaint.2015.01.027, 2015.

Park, S. B., Knohl, A., Migliavacca, M., Thum, T., Vesala, T., Peltola, O., Mammarella, I., Prokushkin, A., Kolle, O., Lavrič, J., Park, S.S. and Heimann, M.: Temperature Control of Spring CO_2 Fluxes at a Coniferous Forest and a Peat Bog in Central Siberia, Atmosphere, 12(8), 984, doi: 10.3390/atmos12080984, 2021.

Parmentier, F. J. W., Van der Molen, M. K., De Jeu, R. A. M., Hendriks, D. M. D. and Dolman, A. J.: CO_2 fluxes and evaporation on a peatland in the Netherlands appear not affected by water table fluctuations, Agr for meteorol, 149(6-7), 1201-1208, doi: 10.1016/j.agrformet.2008.11.007, 2009.

Pavelka, M., Acosta, M., Marek, M. V., Kutsch, W. and Janous, D.: Dependence of the Q_{10} values on the depth of the soil temperature measuring point, Plant Soil, 292(1), 171-179, doi: 10.1007/s11104-007-9213-9, 2007.

Peel, M. C., Finlayson, B. L., and McMahon, T. A.: Updated world map of the Köppen-Geiger climate classification, Hydrol. Earth Syst. Sci., 11, 1633–1644, doi: 10.5194/hess-11-1633-2007, 2007.

Petrescu, A. M. R., Lohila, A., Tuovinen, J. P., Baldocchi, D. D., Desai, A. R., Roulet, N. T., Vesala, T., Dolman, A., J., Oechel, W.C., Marcolla, B., Friborg, T., Rinne, J., Matthes, J.H., Merbold, L., Meijide, A., Kiely, G., Sottocornola, M., Sachs, T., Zona, D., Varlagin, A., Lai, D.Y.F., Veenendaal, E., Parmentier, F.-J.W., Skiba, U., Lund, M., Hensen, A., van Huissteden, J., Flanagan, L.B., Shurpali, N.J., Grünwald, T., Humphreys, E.R., Jackowicz-Korczyński, M., Aurela, M.A., Laurila, T., Grüning, C., Corradi, C.A.R., Schrier-Uijl, A.P., Christensen, T.R., Tamstorf, M.P., Mastepanov, M., Martikainen, P.J., Verma, S.B., Bernhofer, C. and Cescatti, A.: The uncertain climate footprint of wetlands under human pressure, Proceedings of the National Academy of Sciences, 112(15), 4594-4599, doi: 10.1073/pnas.1416267112, 2015.

Piao, S., Ciais, P., Friedlingstein, P., Peylin, P., Reichstein, M., Luyssaert, S., Margolis, H., Fang, J., Barr, A., Chen, A., Grelle, A., Hollinger, D.Y., Laurila, T., Lindroth, A., Richardson, A.D., Vesala, T.: Net carbon dioxide losses of northern ecosystems in response to autumn warming, Nature, 451(7174), 49-52, doi: 10.1038/nature06444, 2008.

Puzachenko, Yu.G. Kotlov, L.P. and Sandlerskiy, R.B.: Analysis of changes of land cover using multispectral remote sensing information in the central forest reserve, Izv. Geogr, 3, 5–18, doi: 10.15356/0373-2444-2014-3-5-18, 2014.

Qiu, C., Zhu, D., Ciais, P., Guenet, B. and Peng, S.: The role of northern peatlands in the global carbon cycle for the 21st century, Global Ecol Biogeogr, 29(5), 956-973, doi: 10.1111/geb.13081, 2020.

Roshydromet: Second Roshydromet Assessment Report on Climate Change and its Consequences in the Russian Federation. General summary., Roshydromet, Moscow, 56, 2014.

Roulet, N. T., Lafleur, P. M., Richard, P. J., Moore, T. R., Humphreys, E. R. and Bubier, J. I. L. L. Contemporary carbon balance and late Holocene carbon accumulation in a northern peatland, Glob Change Biol, 13(2), doi: 10.1111/j.1365-2486.2006.01292.x, 397-411, 2007.

Schulze, E. D., Vygodskaya, N. N., Tchebakova, N. M., Czimczik, C. I., Kozlov, D. N., Lloyd, J., Sidorov, K.N., Varlagin, A.V. and Wirth, C.: The Eurosiberian transect: an introduction to the experimental region, Tellus B, 54(5), 421-428, doi: 10.3402/tellusb.v54i5.16678, 2002.

Syed, K. H., Flanagan, L. B., Carlson, P. J., Glenn, A. J. and Van Gaalen, K. E.: Environmental control of net ecosystem CO_2 exchange in a treed, moderately rich fen in northern Alberta, Agr for meteorol, 140(1-4), 97-114, doi: 10.1016/j.agrformet.2006.03.022, 2006.

Sulman, B. N., Desai, A. R., Cook, B. D., Saliendra, N., and Mackay, D. S.: Contrasting carbon dioxide fluxes between a drying shrub wetland in Northern Wisconsin, USA, and nearby forests, Biogeosciences, 6, 1115–1126, doi: 10.5194/bg-6-1115-2009, 2009.

Sulman, B. N., Desai, A. R., Saliendra, N. Z., Lafleur, P. M., Flanagan, L. B., Sonnentag, O., Mackay D.S., Barr, A.G. van der Kamp, G.: CO_2 fluxes at northern fens and bogs have opposite responses to inter-annual fluctuations in water table, Geophys Res Lett, 37(19), doi: 10.1029/2010GL044018, 2010.

Tchebakova, N. M., Vygodskaya, N. N., Arneth, A., Marchesini, L. B., Kurbatova, Y. A., Parfenova, E. I., Valentini, R., Verkhovets, S. V., Vaganov E. A., Schulze, E. D.: Energy and mass exchange and the productivity of main Siberian ecosystems (from Eddy covariance measurements). 2. carbon exchange and productivity., Biology bull, 42(6), 579-588, doi: 10.1134/S1062359015660024, 2015.

RIHMI-WDC database (http://aisori-m.meteo.ru).

Tanja, S., Berninger, F., Vesala, T., Markkanen, T., Hari, P., Mäkelä, A., Ilvesniemi, H., Hänninen, H., Nikinmaa, E., Huttula, T., Laurila, T., Aurela, M., Grelle, A., Lindroth, A., Arneth, A., Shibistova, O. and Lloyd, J.: Air temperature triggers the recovery of evergreen boreal forest photosynthesis in spring, Glob Change Biol, 9(10), 1410-1426, doi: 10.1046/j.1365-2486.2003.00597.x, 2003.

Ueyama, M., Iwata, H. and Harazono, Y.: Autumn warming reduces the CO_2 sink of a black spruce forest in interior Alaska based on a nine-year eddy covariance measurement, Glob Change Biol, 20(4), 1161-1173, doi: 10.1111/gcb.12434, 2014.

Urban SIS D4.3 Indicators for urban assessments, C3S_441 Lot3 Urban SIS, D4.3, Swedish Meteorological and Hydrological Institute, 55 pp., 2018.

Vompersky, S. E., Sirin, A. A., Sal'nikov, A. A., Tsyganova, O. P. and Valyaeva, N. A.: Estimation of forest cover extent over peatlands and paludified shallow-peat lands in Russia, Contemporary Problems of Ecology, 4(7), 734-741, doi: 10.1134/S1995425511070058, 2011.

Vygodskaya, N. N., Schulze, E. D., Tchebakova, N. M., Karpachevskii, L. O., Kozlov, D., Sidorov, K. N., Panfyorov, M. I., Abrazko, M. A., Shaposhnikov, E. S., Solnzeva, O. N., Minaeva, T. Y., Jeltuchin, A. S., Wirth, C. and Pugachevskii, A. V.: Climatic control of stand thinning in unmanaged spruce forests of the southern taiga in European Russia, Tellus B, 54(5), 443-461, doi: 10.3402/tellusb.v54i5.16680, 2002.

Walker, A. P., Carter, K. R., Gu, L., Hanson, P. J., Malhotra, A., Norby, R. J., Sebestyen, S.D., Wullschleger, S.D., Weston, D. J.: Biophysical drivers of seasonal variability in Sphagnum gross primary production in a northern temperate bog, Journal of Geophysical Research: Biogeosciences, 122(5), 1078-1097, doi: 10.1002/2016JG003711, 2017.

Weedon, J. T., Aerts, R., Kowalchuk, G. A., van Logtestijn, R., Andringa, D. and van Bodegom, P. M.: Temperature sensitivity of peatland C and N cycling: does substrate supply play a role?, Soil Biology and Biochemistry, 61, 109-120, doi: 10.1016/j.soilbio.2013.02.019, 2013.

Welp, L. R., Randerson, J. T. and Liu, H. P.: The sensitivity of carbon fluxes to spring warming and summer drought depends on plant functional type in boreal forest ecosystems, Agr for meteorol, 147(3-4), 172-185, doi: 10.1016/j.agrformet.2007.07.010, 2007.

Wieder, R. K. and Vitt, D. H. (Eds.): Boreal peatland ecosystems (Vol. 188), Springer Science & Business Media, 436 pp., 2006.

Willmott, C. J. and Feddema, J. J.: A more rational climatic moisture index, The Professional Geographer, 44(1), 84-88, doi: 10.1111/j.0033-0124.1992.00084.x, 1992.

Wutzler, T., Lucas-Moffat, A., Migliavacca, M., Knauer, J., Sickel, K., Šigut, L., Menzer, O., and Reichstein, M.: Basic and extensible post-processing of eddy covariance flux data with REddyProc, Biogeosciences, 15, 5015–5030, doi: 10.5194/bg-15-5015-2018, 2018.

Yu, Z. C.: Northern peatland carbon stocks and dynamics: a review, Biogeosciences, 9, 4071–4085, doi: 10.5194/bg-9-4071-2012, 2012.

Zagirova, S. V., Mikhailov, O. A. and Schneider, J.: Carbon dioxide, heat and water vapor exchange in the boreal spruce and peatland ecosystems., Theoretical and Applied Ecology, (3), 12-20, doi: 10.25750/1995-4301-2019-3-012-020, 2019.

Zięba, A., Ramza, P.: Standard deviation of the mean of autocorrelated observations estimated with the use of the autocorrelation function estimated from the data, Metrology and Measurement Systems, 18(4), 529-542, 2011.